JOURNAL OF THE AERONAUTICAL SCIENCES

VOLUME 10 FEBRUARY, 1943 NUMBER 2

Three-Dimensional Wing Flutter Analysis

ALEXANDER H. FLAX*

Curtis-Wright Corporation

ABSTRACT

A set of equations is derived for the flutter of a wing-aileron system in three dimensions using methods familiar to the average engineer. The aerodynamic force coefficients are obtained by strip integration of two-dimensional coefficients. The results are presented in a form suitable for direct calculation by assuming that the fundamental vibration modes of the wing in bending and torsion may be used to represent the corresponding displacements of the wing in the flutter motion. The validity of the assumption made is discussed.

Empirical weighting methods commonly used in two-dimensional analyses to account for three-dimensional effects are considered in the light of the results obtained in the paper. Approximate equations are given for the correction of coupled frequencies obtained in still air vibration tests to the "uncoupled" frequencies desired for flutter analysis. The corrections for the effects of the apparent inertia of the air are also included.

INTRODUCTION

THE PRESENT TRENDS toward higher speeds and lighter structures have made flutter considerations increasingly critical in the design of structural components. The reduction of the three-dimensional wing structure to an analogous two-dimensional structure, which has in the past been the most commonly used method of analysis, has proved to be unsatisfactory for many practical problems. Local variations in weight, moment of inertia, and c.g. location have made the choice of suitable two-dimensional parameters extremely questionable. Large local variations of this type frequently arise in wings that are used to carry fuel or armament. Arbitrary methods of weighting parameters have also proved objectionable, because these methods have often been based on unsound assumptions (as will be shown later).

A completely satisfactory solution of the three-dimensional flutter problem can be obtained only by the development of a dynamically and aerodynamically sound theory for flutter in three dimensions. Unfortunately, no complete solution of the aerodynamic problem for a vibrating wing of finite aspect ratio is yet available. A partial solution (no aileron forces are considered) is given in reference 9, but it seems to be too cumbersome for adaptation to practical analysis. Thus, at present, all consideration of aerodynamic forces on the wing must be based on strip theory—that is, the forces on each spanwise element of wing are computed by assuming that the flow there is independent of the fluid motion at all other points on the wing. This assumption involves neglecting the induced velocities caused by the free and trailing vortices all along the span.

Lyon[8] states that the effects of these induced velocities is not as great in a periodic motion of the wing as in a steady motion. This is attributed to the fact that in a periodic motion the successive free and trailing vortices are of opposite sign, and their induced velocities tend to cancel one another out except in the immediate neighborhood of any given vortex. Thus, in a vibrating wing, the effect of finite span will be due mainly to vortices immediately behind the wing.

The most serious errors occur near the tip, as is pointed out by Cicala[9]. This is to be expected, because not only are the trailing vortices largest near the tip but also, in a wing vibrating near the fundamental mode, the amplitudes, which determine the aerodynamic forces, are the largest near the tip. The induced velocities tend to reduce the lift on the wing and are equivalent to an aerodynamic damping. The effect is to increase the flutter speed so that neglect of span effects is conservative.

For wings of large aspect ratio, neglect of aerodynamic span effects is not likely to lead to large errors in calculated flutter speeds as was pointed out by Theodorsen and Garrick[7]. For tail surfaces, however, where the aspect ratio may be three or lower, the error may be quite large. This is borne out by the fact that the flutter modes involving tail surface bending torsion have led to flutter speeds, when calculated by conventional methods that had proved to be successful on wings, which were far lower than practical ex-

Received August 4, 1942.

* Structures Engineer, Airplane Division.

perience would admit. For tail surfaces, it may be possible to apply empirical corrections to the aerodynamic force coefficients to account for aspect ratio effects. Such phases of the problem as have already been solved (presented in references 8 and 9) should be of considerable value in determining the empirical corrections. The equations set up in this paper allow for inclusion of any such corrections to the local aerodynamic force coefficients.

A rigorous solution of the problem of three-dimensional flutter insofar as the dynamic and elastic phases are concerned offers no fundamental theoretic difficulties, since the methods of classic mechanics are sufficient to solve the problem. The difficulties involved are purely those of practical computation. The wing in three dimensions constitutes a system with an infinite number of degrees of freedom. If all wing displacements are assumed to consist of bending displacements, h, of the elastic axis, and torsional displacements, α, about the elastic axis, then the deformation of the wing may be described as a function of time and spanwise location by the two infinite series (if a solution that is a sinusoidal function of time is assumed):

$$h(x, t) = a_1 e^{i(\omega t)} f_1(x) + a_2 e^{i(\omega t + \phi_2)} f_2(x) + \ldots .$$

$$\alpha(x, t) = b_1 e^{i(\omega t + \theta_1)} g_1(x) + b_2 e^{i(\omega t + \theta_2)} g_2(x) \ldots \ldots .$$

Where the a's and b's are constants, the f's and g's are arbitrary functions for the shape of the displacement curves that satisfy the boundary conditions in bending and torsion, respectively, and the θ's and ϕ's represent the time phase relationships between the various terms; ω represents the natural frequency of the periodic motion. Each term in the series represents a degree of freedom, and the accuracy of any work depends on the number of terms employed. The wing motion could probably be sufficiently well described by the use of two or three terms in each series, but when at least one degree of freedom is added to describe aileron motion, a total of from five to seven degrees of freedom results. Inasmuch as solution of the flutter problem involves a trial-and-error solution of a determinant of order equal to the number of degrees of freedom, such a procedure is seen to be unsuitable for routine analysis.

An alternative method proposed by Lombard,[1] as well as by various British investigators, is to use only two degrees of freedom to describe the displacement of the wing, one for bending and one for torsion. The displacement curves are assumed to be the same as those obtained from vibration of the wing in the fundamental modes for bending and torsion. These curves may be obtained either from ground vibration tests or by calculation.[11] This procedure implies that flutter occurs in the fundamental mode. This, of course, is not necessarily true, but for wings having a damping coefficient comparable to that of most modern metal wings, the error will not be serious as pointed out by Theodorsen and Garrick.[7] In this paper, the fundamental modes of bending and torsion will be assumed to be the displacement curves in the flutter motion, in order that the number of degrees of freedom may be limited to three.

Several papers on three-dimensional flutter analysis have already been published; those of Lombard,[1] Loring,[2] and Bleakney[3] are of particular interest. Lombard has derived a set of three-dimensional equations using assumed deflection curves. He has not, however, employed the commonly used notation of references 6 and 7 and, further, his analysis does not include aileron effects. Loring and Bleakney have both derived sets of general equations applicable to any number of degrees of freedom which undoubtedly constitute important contributions to the basic theory of flutter in three dimensions. Loring, however, has employed instruments of analysis, such as Lagrange's equations and matrices, which can hardly be regarded as part of the equipment of the average aeronautical engineer. Bleakney too has employed a method of derivation not familiar to the average engineer. The results of both these papers have not been developed to the point where immediate use for routine calculations is possible, mainly because both authors wished to allow for treatment of a large variety of problems involving many possible degrees of freedom.

It is the purpose of this paper to develop, by using principles of mechanics and mathematics within the scope of the average engineer, a method for three-dimensional wing flutter analysis in three degrees of freedom. The nomenclature of references 6 and 7 is employed wherever possible.

The Equations of Motion

Consider a spanwise element of wing and the forces acting upon it as in Fig. 1. The case of torsional motion is chosen as typical. If α is the angle of twist,

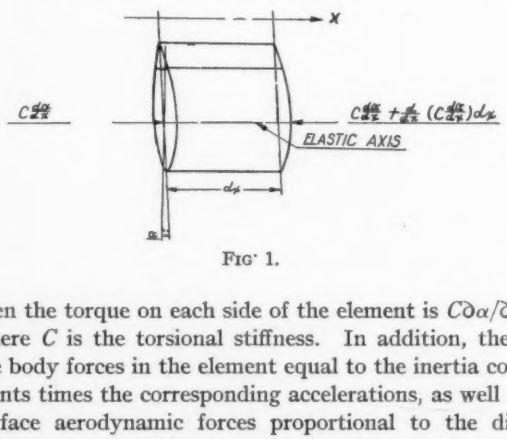

Fig. 1.

then the torque on each side of the element is $C\partial\alpha/\partial x$, where C is the torsional stiffness. In addition, there are body forces in the element equal to the inertia constants times the corresponding accelerations, as well as surface aerodynamic forces proportional to the displacements, velocities, and accelerations of the element. The body inertia forces (per unit length) are given on page 9 of reference 6 as:

$$I_\alpha \frac{\partial^2 \alpha}{\partial t^2} + [I_\beta + b(c-a)\,S_\beta] \frac{\partial^2 \beta}{\partial t^2} + S_\alpha \frac{\partial^2 h}{\partial t^2}$$

Assuming simple harmonic motion for the displacements,

$$\begin{aligned} \alpha &= \alpha' e^{i\omega t} \\ \beta &= \beta' e^{i(\omega t + \phi_1)} \\ h &= h' e^{i(\omega t + \phi_2)} \end{aligned}$$

where α', β', and h' are functions of spanwise distance from the wing root, x, alone and represent the temporal maxima of the displacements. ϕ_1 and ϕ_2 are the phase angles by which the aileron and bending displacements, respectively, lead the torsional motion. Then

$$\begin{aligned} \partial^2\alpha/\partial t^2 &= -\omega^2\alpha \\ \partial^2\beta/\partial t^2 &= -\omega^2\beta \\ \partial^2 h/\partial t^2 &= -\omega^2 h \end{aligned}$$

Summing all moments about the elastic axis of the element, and noting that since time has been eliminated as a variable the partial derivatives may be replaced by total derivatives leads to

$$-\frac{d}{dx}\left(C\frac{d\alpha}{dx}\right) - \omega^2 I_\alpha \alpha - \omega^2[I_\beta + b(c-a)S_\beta]\beta - \omega^2 S_\alpha h - M_\alpha = 0 \tag{1}$$

where M_α is the moment about the elastic axis of the aerodynamic forces. This will be treated later. Multiplying through Eq. (1) by $\alpha/2$ and integrating with respect to x from 0 to l, where 0 is at the root of the wing and l at the tip, gives

$$-\int_0^l \frac{\alpha}{2}\frac{d}{dx}\left(c\frac{d\alpha}{dx}\right)dx - \omega^2\int_0^l I_\alpha \frac{\alpha^2}{2}\,dx - \omega^2\int_0^l [I_\beta + b(c-a)]\,\frac{\beta\alpha}{2}\,dx - \omega^2\int_0^l S_\alpha \frac{h\alpha}{2}\,dx - \int_0^l M_\alpha \frac{\alpha}{2}\,dx = 0 \tag{2}$$

The first term of Eq. (2) may be further reduced by partial integration using the formula

$$\int_{x_1}^{x_2} u\frac{dv}{dx}\,dx = |u\cdot v|_{x_1}^{x_2} - \int_{x_1}^{x_2} v\frac{du}{dx}\,dx$$

Let $$\alpha/2 = u \text{ and } \frac{d}{dx}\left(C\frac{d\alpha}{dx}\right) = \frac{dv}{dx}$$

Then $$\int_0^l \frac{\alpha}{2}\frac{d}{dx}\left(C\frac{d\alpha}{dx}\right)dx = \left|\frac{\alpha}{2}C\frac{d\alpha}{dx}\right|_0^l - \int_0^l \frac{C}{2}\left(\frac{d\alpha}{dx}\right)^2 dx$$

Since $\alpha = 0$ at $x = 0$ and $d\alpha/dx = 0$ at $x = l$, the first term on the right side of the equation above drops out, giving:

$$\int_0^l \frac{\alpha}{2}\frac{d}{dx}\left(C\frac{d\alpha}{dx}\right)dx = -\int_0^l \frac{C}{2}\left(\frac{d\alpha}{dx}\right)^2 dx \tag{3}$$

Substituting Eq. (3) into Eq. (2)

$$\int_0^l \frac{C}{2}\left(\frac{d\alpha}{dx}\right)^2 dx - \omega^2\int_0^l I_\alpha\frac{\alpha^2}{2}\,dx - \omega^2\int_0^l [I_\beta + b(c-a)S_\beta]\frac{\beta\alpha}{2}\,dx - \omega^2\int_0^l S_\alpha\frac{h\alpha}{2}\,dx - \int_0^l M_\alpha\frac{\alpha}{2}\,dx = 0 \tag{4}$$

The expressions $h = h_t f_1(x)$ and $\alpha = \alpha_t f_2(x)$ may now be substituted in Eq. (4), where f_1 and f_2 are the fundamental vibration modes in bending and torsion, respectively, and the subscript t indicates tip value of the displacements. Eq. (4) becomes after division by $\int_0^l (I_\alpha \alpha^2/2)dx$,

$$(\omega_\alpha{}^2 - \omega^2)\alpha_t - \omega^2\beta\frac{\int_0^l [I_\beta + b(c-a)S_\beta]f_2 dx}{\int_0^l I_\alpha f_2{}^2 dx} - \omega^2 h_t\frac{\int_0^l S_\alpha f_1 f_2 dx}{\int_0^l I_\alpha f_2{}^2 dx} - \frac{1/\alpha_t\int_0^l M_\alpha \alpha dx}{\int_0^l I_\alpha f_2{}^2 dx} = 0 \tag{4a}$$

since the expression

$$\int_0^l C[(f_2')^2/2]dx \Big/ \int_0^l (I_\alpha f_2{}^2/2)dx = \omega_\alpha{}^2$$

where ω_α is the fundamental torsional frequency involving the f_2 mode (see page 185, reference 5).

By similar treatment of the equations of equilibrium for aileron moments and for bending forces as given on page 9 of reference 6, two additional relationships are obtained.

The equation for aileron motion becomes

$$(\omega_\beta{}^2 - \omega^2)\beta - \frac{\omega^2\alpha_t}{I_\beta\gamma l}\int_{\gamma_1 l}^{\gamma_2 l} I_\beta f_2 dx - \frac{\omega^2\alpha_t}{I_\beta\gamma l}\int_{\gamma_1 l}^{\gamma_2 l} b(c-a)S_\beta f_2 dx - \frac{\omega^2 h_t}{I_\beta\gamma l}\int_{\gamma_1 l}^{\gamma_2 l} S_\beta f_1 dx - \frac{1}{I_\beta\gamma l}\frac{1}{\beta}\int_{\gamma_1 l}^{\gamma_2 l} M_\beta\beta dx = 0 \tag{4b}$$

where γl is the length of the aileron and $\gamma_1 l$ and $\gamma_2 l$ are the distances from the wing root to the inboard and outboard ends of the aileron, respectively.

The bending equation leads to:

$$(\omega_h{}^2 - \omega^2)h_t - \omega^2\beta\frac{\int_0^l S_\beta f_1 dx}{\int_0^l M f_1{}^2 dx} - \omega^2\alpha_t\frac{\int_0^l S_\alpha f_2 f_1 dx}{\int_0^l M f_1{}^2 dx} - \frac{1}{h_t}\frac{\int_0^l P h dx}{\int_0^l M f_1{}^2 dx} = 0 \tag{4c}$$

Aerodynamic Forces

Theodorsen on page 9 of reference 6 presents the equation for the forces and moments on a unit strip of airfoil as linear functions of the displacements.

These equations may be expressed in the following form (first suggested by Loring[2]):

$$\left.\begin{aligned} P &= -\pi\rho\omega^2 b^2(A_{ch}\,h + A_{c\alpha}\,b\alpha + A_{c\beta}\,b\beta) \\ M_\alpha &= -\pi\rho\omega^2 b^3(A_{ah}\,h + A_{a\alpha}\,b\alpha + A_{a\beta}\,b\beta) \\ M_\beta &= -\pi\rho\omega^2 b^3(A_{bh}\,h + A_{b\alpha}\,b\alpha + A_{b\beta}\,b\beta) \end{aligned}\right\} \tag{5}$$

where A_{ij} is equal to $R_{ij} + iI_{ij}$ on page 12 of reference 6 with all mass and elastic terms omitted (terms containing K or Ω). Then,

$$-\frac{\frac{1}{\alpha_t}\int_0^l M_\alpha\alpha dx}{\int_0^l I_\alpha f_2{}^2 dx} = \frac{\pi\rho b_0{}^3\omega^2 l}{\int_0^l I_\alpha f_2{}^2 dx}\left[\frac{h_t}{l}\int_0^l\left(\frac{b}{b_0}\right)^3 A_{ah}f_1 f_2 dx + \frac{\alpha_t b_0}{l}\int_0^l\left(\frac{b}{b_0}\right)^4 A_{a\alpha}f_2{}^2 dx + \frac{\beta b_0}{l}\int_{\gamma_1 l}^{\gamma_2 l}\left(\frac{b}{b_0}\right)^4 A_{a\beta}f_2 dx\right] \tag{6}$$

Also

$$-\frac{1}{I_\beta\gamma l}\frac{1}{\beta}\int_{\gamma_1 l}^{\gamma_2 l} M_\beta\beta dx = \frac{\pi\rho b_0{}^3\omega^2 l}{I_\beta\gamma l}\left[\frac{h_t}{l}\int_{\gamma_1 l}^{\gamma_2 l}\left(\frac{b}{b_0}\right)^3 A_{bh}f_1 dx + \frac{\alpha_t b_0}{l}\int_{\gamma_1 l}^{\gamma_2 l}\left(\frac{b}{b_0}\right)^4 A_{b\alpha}f_2 dx + \frac{\beta b_0}{l}\int_{\gamma_1 l}^{\gamma_2 l}\left(\frac{b}{b_0}\right)^4 A_{b\beta}dx\right] \tag{7}$$

Finally

$$-\frac{\frac{1}{h_t}\int_0^l P h dx}{\int_0^l M f_1{}^2 dx} = \frac{\pi\rho b_0{}^2\omega^2 l}{\int_0^l M f_1{}^2 dx}\left[\frac{h_t}{l}\int_0^l\left(\frac{b}{b_0}\right)^2 A_{ch}f_1{}^2 dx + \frac{\alpha_t b_0}{l}\int_0^l\left(\frac{b}{b_0}\right)^3 A_{c\alpha}f_1 f_2 dx + \frac{\beta b_0}{l}\int_{\gamma_1 l}^{\gamma_2 l}\left(\frac{b}{b_0}\right)^3 A_{c\beta}f_1 dx\right] \tag{8}$$

It will be noted that in Eqs. (6), (7), and (8), an arbitrary reference semichord b_0 has been introduced. An examination of the equations will disclose that the particular chord chosen has no effect whatever on the overall values of the functions on the right side of Eqs. (6), (7), and (8). The A's for any given wing are functions of $V/b\omega$ where b is the local semichord at any station. In solving for the flutter speed values of the aerodynamic force, integrals will be required for several values of $V/b_0\omega$. This necessitates recomputing the integrals several times graphically because the A's are complicated functions of $V/b\omega$, which of course varies from station to station. The difficulties involved in such calculation may be circumvented by using simple approximate expressions for the A's. These expressions may be obtained by fitting the curves of A versus $V/b\omega$ for the given wing obtained from reference 6. The A value may be broken down to real and imaginary parts, so that $A = A_R + iA_I$. It has been found that in the range from $V/b\omega = 0$ to $V/b\omega = 7$, the value of either the real or imaginary part of A may be satisfactorily approximated by (at most) a parabolic function. Thus,

$$A_R = A_{R0} + m_R\,(V/b\omega) + n_R(V/b\omega)^2$$

Substituting into an integral of the form: $I_R = \int_0^l (b/b_0)^n A_R f(x)dx$ gives

$$I_R = \int_0^l\left(\frac{b}{b_0}\right)^n\left[A_{R0} + m_R\left(\frac{V}{b\omega}\right) + n_R\left(\frac{V}{b\omega}\right)^2\right]f(x)dx$$

which may be written as

$$I_R = A_R\int_0^l\left(\frac{b}{b_0}\right)^n f(x)dx + m_R\left(\frac{V}{b_0\omega}\right)\int_0^l\left(\frac{b}{b_0}\right)^{n-1} f(x)dx + n_R\left(\frac{V}{b_0\omega}\right)^2\int_0^l\left(\frac{b}{b_0}\right)^{n-2} f(x)dx \tag{9}$$

The integrals in Eq. (9) do not vary with $V/b_0\omega$ and need only be computed once. Thus, the computation of the aerodynamic force terms for various values of $V/b_0\omega$, once the integrals are initially computed, is no more difficult than in the two-dimensional case.

In some cases, especially where the variation of b along the span is not great, it may be possible to regard the A's as constant over the entire span and to compute them on the basis of the value of $V/b\omega$ at the three-quarter semispan section. A simplification of this type seems especially justified because the A values are themselves necessarily approximate, neglecting as they do the effects of finite span. Lombard[1] makes an assumption of this type in his equations. Further work on this matter is necessary with a view toward determining a simple yet close approximation, possibly even including span effects in a rough manner.

Solution of the Stability Determinant

Substituting Eqs. (6), (7), and (8) into Eqs. (4a), (4b), and (4c), the equations of motion are reduced to the form

$$\left.\begin{aligned} A\alpha_t + B\beta + Ch_t &= 0 \text{ (torsion)} \\ D\alpha_t + E\beta + Fh_t &= 0 \text{ (aileron)} \\ G\alpha_t + H\beta + Ih_t &= 0 \text{ (bending)} \end{aligned}\right\} \tag{10}$$

The coefficients of α_t, β, h_t are complex functions of the physical parameters of the airplane, ω_α/ω and $V/b_0\omega$. Damping coefficients g_α, g_β, and g_h may be introduced in a manner similar to that used in reference 7. The following symbols are employed in the coefficients:

$$M_r = \int_0^l M f_1^2 dx \qquad I_\beta' = I_\beta \gamma l \qquad I_r = \int_0^l I_\alpha f_2^2 dx$$

Eqs. (4a), (4b) and (4c) are divided through by ω^2, and the coefficients become,

$$\left.\begin{aligned}
A &= \left[\frac{\omega_\alpha^2}{\omega^2}(1 + ig_\alpha) - 1\right] + \frac{\pi\rho b_0^3 l}{I_r}\left[\frac{b_0}{l}\int_0^l \left(\frac{b}{b_0}\right)^4 A_{a\alpha} f_2^2 dx\right] \\
B &= -\frac{\int_{\gamma l}^{\gamma l} [I_\beta + b(c-a)S_\beta] f_2 dx}{I_r} + \frac{\pi\rho b_0^3 l}{I_r}\left[\frac{b_0}{l}\int_{\gamma l}^{\gamma l}\left(\frac{b}{b_0}\right)^4 A_{a\beta} f_2 dx\right] \\
C &= -\frac{\int_0^l S_\alpha f_1 f_2 dx}{I_r} + \frac{\pi\rho b_0^3 l}{I_r}\left[\frac{1}{l}\int_0^l \left(\frac{b}{b_0}\right)^3 A_{ah} f_1 f_2 dx\right] \\
D &= -\frac{\int_{\gamma l}^{\gamma l} [I_\beta + b(c-a)S_\beta] f_2 dx}{I_\beta'} + \frac{\pi\rho b_0^3 l}{I_\beta'}\left[\frac{b_0}{l}\int_{\gamma l}^{\gamma l}\left(\frac{b}{b_0}\right)^4 A_{b\alpha} f_2 dx\right] \\
E &= \left[\frac{\omega_\beta^2}{\omega^2}(1 + ig_\beta) - 1\right] + \frac{\pi\rho b_0^3 l}{I_\beta'}\left[\frac{b_0}{l}\int_{\gamma l}^{\gamma l}\left(\frac{b}{b_0}\right)^4 A_{b\beta} dx\right] \\
F &= -\frac{\int_{\gamma l}^{\gamma l} S_\beta f_1 dx}{I_\beta'} + \frac{\pi\rho b_0^3 l}{I_\beta'}\left[\frac{1}{l}\int_{\gamma l}^{\gamma l}\left(\frac{b}{b_0}\right)^3 A_{bh} f_1 dx\right] \\
G &= -\frac{\int_0^l S_\alpha f_1 f_2 dx}{M_r} + \frac{\pi\rho b_0^2 l}{M_r}\left[\frac{b_0}{l}\int_0^l \left(\frac{b}{b_0}\right)^3 A_{c\alpha} f_1 f_2 dx\right] \\
H &= -\frac{\int_{\gamma l}^{\gamma l} S_\beta f_1 dx}{M_r} + \frac{\pi\rho b_0^2 l}{M_r}\left[\frac{b_0}{l}\int_{\gamma l}^{\gamma l}\left(\frac{b}{b_0}\right)^3 A_{c\beta} f_1 dx\right] \\
I &= \left[\frac{\omega_h^2}{\omega^2}(1 + ig_\beta) - 1\right] + \frac{\pi\rho b_0^2 l}{M_r}\left[\frac{1}{l}\int_0^l \left(\frac{b}{b_0}\right)^2 A_{ch} f_1^2 dx\right]
\end{aligned}\right\} \tag{10}$$

Eqs. (10) will all be satisfied only when the determinant of the coefficients is equal to zero or

$$\begin{vmatrix} ABC \\ DEF \\ GHI \end{vmatrix} = 0 \tag{11}$$

This leads to the relationship

$$AEI + BFG + CDH - CEG - AFH - BDI = 0 \tag{12}$$

The unknowns in Eq. (12) are $V/b_\alpha\omega$ and ω/ω_α; the real and imaginary parts of Eq. (12) must each independently be equal to zero so that two independent equations are provided for determination of the two unknowns. The procedure followed is to assume several values of $V/b_0\omega$ and to solve for ω/ω_α for each value from both the real and imaginary equations. Two curves of $V/b_0\omega$ versus ω/ω_α are thus obtained, one from the real part of Eq. (12) and the other from the imaginary part of Eq. (12). The values of $(V/b_0\omega)_s$ and $(\omega/\omega_\alpha)_s$ at the intersections of the curves represent critical flutter speeds. The flutter speeds may be found as

$$V = (V/b_0\omega)_s(\omega/\omega_\alpha)_s b_0\omega_\alpha \tag{13}$$

Relation to Two-Dimensional Analysis

It will be of some interest to compare the results of the three-dimensional analysis with some of the commonly used arbitrary methods for putting three-dimensional effects into the two-dimensional methods. Consider the commonly used weighting formulas as given in reference 10.

$$\overline{M} = \frac{\int_0^l Mh\,dy}{\int_0^l h\,dy} \tag{14}$$

where M is the mass per unit length, and

$$\bar{\rho}^2 = \int_0^l \rho^2\alpha\,dy / \int_0^l \alpha\,dy \tag{14a}$$

and ρ is the radius of gyration about the c.g. expressed in per cent of chord.

Examination of Eq. (4c) shows that M should be weighted as h^2 rather than as h. Weighting in proportion to h tends to overemphasize inboard parameters sometimes leading to appreciable errors. The same argument may be seen to hold for Eq. (14a) from Eq. (4a). Even if the weighting is carried out as the square of the deflection curves, discrepancies still remain. For instance, the value of x_β actually must be weighted differently for use in the different equations. This can be seen in Eqs. (4a), (4b), and (4c). Terms in S_β appear as follows:

$$InH/\int_{\gamma_1}^{\gamma_2} S_\beta f_1\,dx/M_r$$

$$InB/\int_{\gamma_1}^{\gamma_2}(c-a)bS_\beta f_2\,dx/I_r$$

$$InF/\int_{\gamma_1}^{\gamma_2} b(c-a)S_\beta f_1\,dx/I_\beta'$$

The two-dimensional theory allows for only one value of x_β unless the analyst rederives the x_β terms and revises the equations.

If the weighted chord is used for the determination of aerodynamic properties, the problem of which power of the chord to use in weighting arises. Examination of aerodynamic terms in the equations of this paper shows variation as the square, cube, and fourth power of the chord in different terms.

The equations of this paper, being three-dimensional, include the effects of partial-span ailerons. Theodorsen and Garrick[7] modify the two-dimensional analysis for this effect by means of a coupling factor ξ, applied only to the aileron equation. The terms D and F indicate that for three degrees of freedom the terms of aileron equation must be modified by two coupling factors, one based on h and the other on α. In addition, the terms giving the aileron effect in the bending and torsion equations must be modified by similar coupling factors as in terms B and H.

It is hoped that this brief discussion will aid in the intelligent choice of two-dimensional parameters for use in various preliminary analyses where a three-dimensional analysis is not justified because of sketchy data.

Ground Vibration Tests

The methods developed in this paper will be of considerable value in interpretation of ground and vibration tests. The tests always give frequencies that represent couplings between bending and torsional motion instead of the fictitious "uncoupled" frequencies desired for use in the flutter equations. In addition, the tests include the effects of apparent air mass which are not desired in the "uncoupled" frequencies. The solution for the "uncoupled" frequencies in terms of the coupled may be obtained from Eqs. (4a) and (4c) set down for $V/b\omega = 0$. Then Eq. (4c) gives

$$\left[\left(\frac{\omega_h}{\omega}\right)^2 - 1\right]h_t - \alpha_t\frac{\int_0^l S_\alpha f_2 f_1\,dx}{\int_0^l M(f_1)^2\,dx} + \frac{\pi\rho b_0^2 l}{\int_0^l M(f_1)^2\,dx}\left[-\frac{h_t}{l}\int_0^l\left(\frac{b}{b_0}\right)^2 f_1^2\,dx + \frac{\alpha_t b_0 a}{l}\int_0^l\left(\frac{b}{b_0}\right)^3 f_1 f_2\,dx\right] = 0 \tag{15}$$

and Eq. (4a) gives

$$\left[\left(\frac{\omega_\alpha}{\omega}\right)^2 - 1\right]\alpha_t - \frac{h_t\int_0^l S_\alpha f_1 f_2\,dx}{\int_0^l I_\alpha(f_2)^2\,dx} + \frac{\pi\rho b_0^3 l}{\int_0^l I_\alpha(f_2)^2\,dx}\left[\frac{h_t a}{l}\int_0^l\left(\frac{b}{b_0}\right)^3 f_1 f_2\,dx - \left(\frac{1}{8}+a^2\right)\frac{\alpha_t b_0}{l}\int_0^l\left(\frac{b}{b_0}\right)^4 (f_2)^2\,dx = 0\right. \tag{15a}$$

The integrals will all be needed in any event for use in the flutter analysis so no additional evaluation of integrals is involved. Then the equations may be written:

$$\left.\begin{aligned}\left[\left(\frac{\omega_h}{\omega}\right)^2 + Q\right] h_t + P\alpha_t = 0 \\ Mh_t + \left[\left(\frac{\omega_\alpha}{\omega}\right)^2 + N\right] \alpha_t = 0\end{aligned}\right\} \quad (16)$$

The determinant of the coefficients of these equations must equal zero in order that they may be satisfied for all values of h_t and α_t. This leads to the equation

$$\left(\frac{\omega}{\omega_h}\right)^2 = \left\{-\left[\left(\frac{\omega_\alpha}{\omega_h}\right)^2 Q + N\right] \pm \sqrt{\left[\left(\frac{\omega_\alpha}{\omega_h}\right)^2 Q + N\right]^2 - 4\left(\frac{\omega_\alpha}{\omega_h}\right)^2 (QN - PM)}\right\} / 2(QN - PM) \quad (17)$$

Thus, two coupled frequencies, ω_1 and ω_2, may be computed from the calculated "uncoupled" frequencies ω_h and ω_α and may be checked against coupled frequencies obtained in the tests. To solve for the "uncoupled" frequencies from the coupled, ω_1 and ω_α are substituted in Eq. (7) for ω, giving two equations in ω_α and ω_h. These are:

$$\left.\begin{aligned}\left(\frac{\omega_h}{\omega_1}\right)^2\left(\frac{\omega_\alpha}{\omega_1}\right)^2 + \left(\frac{\omega_\alpha}{\omega_1}\right)^2 Q + \left(\frac{\omega_h}{\omega_1}\right)^2 N + QN - PM = 0 \\ \left(\frac{\omega_h}{\omega_2}\right)^2\left(\frac{\omega_\alpha}{\omega_2}\right)^2 + \left(\frac{\omega_\alpha}{\omega_2}\right)^2 Q + \left(\frac{\omega_h}{\omega_2}\right)^2 N + QN - PM = 0\end{aligned}\right\} \quad (18)$$

Values of ω_h are assumed and ω_α is calculated from each equation. Two curves are plotted and the point of intersection represents the solution.

References

[1] Lombard, A. E., Jr., *An Investigation of the Conditions for Occurrence of Flutter in Aircraft*, Thesis, California Institute of Technology, 1939.

[2] Loring, S. J., *General Approach to the Flutter Problem*, S.A.E. Journal, Vol. 49, No. 2, pp. 345–356, August, 1941.

[3] Bleakney, W. M., *Three-Dimensional Flutter Analysis*, Journal of the Aeronautical Sciences, Vol. 9, No. 2, pp. 56–63, December, 1941.

[4] Frazer, R. A., and Duncan, W. J., *The Flutter of Aeroplane Wings*, R. & M. 1155, 1929.

[5] Den Hartog, J. P., *Mechanical Vibrations;* McGraw-Hill Book Company, Inc., New York, 1941.

[6] Theodorsen, T., *General Theory of Aerodynamic Instability and the Mechanism of Flutter*, N.A.C.A. T.R. No. 496, 1935.

[7] Theodorsen, T., and Garrick, I., *Mechanism of Flutter*, N.A.C.A. T.R. No. 685, 1940.

[8] Lyon, H. M., *A Review of Theoretical Investigation of the Aerodynamic Forces on a Wing in Non-Uniform Motion*, R. & M. 1786, 1937.

[9] Cicala, P., *Comparison of Theory with Experiment in the Phenomenon of Wing Flutter*, N.A.C.A. T.M. No. 887, 1939.

[10] *Parallel Axes Control Surface Binary Flutter*, C.A.A. Engineering Section Report No. 24, 1941.

[11] Burgess, *Frequency of Cantilever Wings in Beam and Torsional Vibration*, N.A.C.A. T.N. No. 746, 1940.

Rate of Climb Calculations

G. OTTEN*

Bandoeng University

Introduction

Frederick C. Phillips[1] has pointed out that in various cases the assumption of zero acceleration along a flight path is not correct and has given an equation by which the rate of climb calculations made in the usual way could be corrected for the error of neglecting the dynamic effect of the acceleration.

It is also generally known that, especially for airplanes of great climbing capacity, the assumption that in the position for climb the lift should be equal to the gross weight causes other inaccuracies in the calculations of the rate of climb.[2]

The correlations that have to be made if no account is taken of the acceleration or the smaller amount of the lift when the airplane climbs will generally be in an opposite direction and partially eliminate each other. While in such calculations the results are not unsatisfactory, decreasing tolerances, increasing engine powers, higher wing and propeller loadings by decreasing drag coefficients make it desirable to look for a better method of calculating the rate of climb.[2]

With the method described below and making use of normal data, the climbing speed of every airplane can be determined with great accuracy without materially increasing the amount of work involved.

Symbols

The following symbols will be used:

F	=	force in general
W	=	gross weight (lbs.)
T	=	thrust (lbs.)
D	=	drag (lbs.)
ρ	=	air mass density
f	=	airplane drag area
q	=	total energy pressure $= \rho V^2/2$
g	=	acceleration of gravity
θ	=	inclination of flight path to horizon (radians)
C	=	flight rate of climb (ft. per sec.)
V	=	air speed
t	=	time (sec.)
A	=	horsepower equivalent (550 ft.lbs. per sec.)
(hp.)	=	engine power
η	=	propulsive efficiency
C_L	=	lift coefficient corrected for the whole airplane, when climbing $= L/qf$
C_D	=	drag coefficient corrected for the whole airplane, when climbing $= D/qf$
C_{Lh}	=	lift coefficient for horizontal flight $= W/qf$
C_{Dh}	=	drag coefficient for horizontal flight
C_C	=	climbing speed coefficient $= CW/qVf$

Received September 1, 1942.

* Lt. Col.; Prof. Dr. of Engineering.

Derivation of the Formulas

The power delivered to the airplane by the propeller $A\eta$ (hp.) can be divided into the power DV necessary to overcome the air resistance, the power WC necessary for climbing, and the power $(VW/g)(dV/dt)$ for the acceleration of the airplane, so that:

$$A\eta(\text{hp.}) = DV + WC + V\,(W/g)(dV/dt) \quad (1)$$

and because $C = V \sin\theta$

$$A\eta(\text{hp.})/V = D + W \sin\theta + (W/g)(dV/dt) \quad (2)$$

As, according to Fig. 1, the forces acting perpendicularly to the direction of the flight path must be in equilibrium:

$$L = W \cos\theta \quad (3)$$

hence,

$$W \sin\theta = \sqrt{(W^2 - L^2)} \quad (4)$$

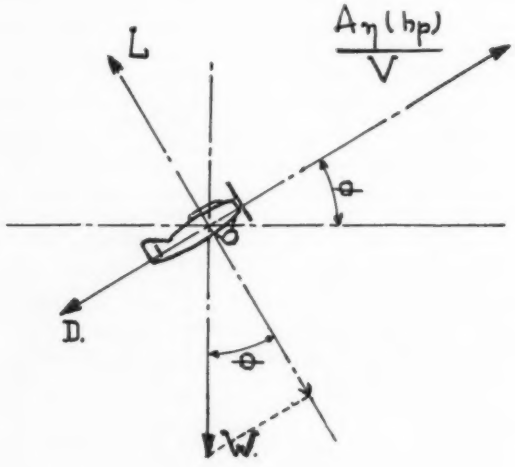

Fig. 1.

Using Eq. (4) and the well-known aerodynamic equations:

$$D = C_D q f \quad (5)$$

and

$$L = C_L q f \quad (6)$$

Eq. (2) may be written in the following form:

$$\frac{A\eta(\text{hp.})}{V} - C_D q f - \left(\frac{W}{g}\right)\left(\frac{dV}{dt}\right) = \sqrt{(W^2 - C_L^2 q^2 f^2)} \quad (7)$$

By squaring both sides of Eq. (7) and rearranging:

$$C_L^2 + C_D^2 - 2C_D\left[\frac{A\eta(\text{hp.})}{Vqf} - \left(\frac{W}{gqf}\right)\left(\frac{dV}{dt}\right)\right] + \left[\frac{A\eta(\text{hp.})}{Vqf} - \left(\frac{W}{gqf}\right)\left(\frac{dV}{dt}\right)\right]^2 - \frac{W^2}{q^2f^2} = 0 \quad (8)$$

Supposing that the airplane is flying at a certain selected altitude with the throttle entirely open and that the engine is giving its maximum power, then Eq. (8) only has terms that are dependent upon a variable V.

Eq. (8) therefore represents a series of circles in the C_L–C_D plane, the centers of which are on the C_D axis.

Further considering the circles, shift the C_L axis in such a way that this axis goes through the points

$$C_D = \frac{A\eta(\text{hp.})}{Vqf} - \left(\frac{W}{gqf}\right)\left(\frac{dV}{dt}\right) \text{ and } C_L = 0 \quad (9)$$

then, by arranging Eq. (8) with the help of

$$C_D = C_{D1} + \frac{A\eta(\text{hp.})}{Vqf} - \left(\frac{W}{gqf}\right)\left(\frac{dV}{dt}\right)$$

the equation for the circles becomes

$$C_L^2 + C_{D1}^2 - (W^2/q^2f^2) = 0 \quad (10)$$

Further, assuming that

$$W = C_{Lh}\, qf \quad (11)$$

in which C_{Lh} is the lift coefficient when flying horizontally at the speed V, Eq. (10) will read as follows:

$$C_L^2 + C_{D1}^2 = C_{Lh}^2 \quad (12)$$

As C_{Lh} is the lift coefficient of the weight W of the airplane and C_L is the coefficient actually used and of the lift L, Eq. (12) gives some idea of the errors that are made by assuming $L = W$.

A circle of the form of Eq. (12) described in the form of Eq. (8) will intersect the C_D–C_L curve of the airplane, the polar curve, in zero, one or more points.

By not considering those intersections that yield a negative lift coefficient and those situated in the area in which the wing is stalling, then, with usable airfoils, only one or zero intersections will be left.

If there are no intersections, it means that no values of C_L and C_D at the chosen speed and acceleration can be found.

If a point of intersection of a circle of the form of Eq. (8) with the polar curve is found, three cases may be represented:

(1) When the value of C_D in the point of intersection of circle and polar curve is greater than the value of C_D in the center of the circle, being $(A\eta(\text{hp.})/Vqf) - (W/gqf)(dV/dt)$, the requirements of Eq. (7) have not been met with; the speed is too high for continuous flight.

(2) When the value of C_D in the point of intersection is equal to the value mentioned in Case (1), Eq. (7) is satisfied only by putting $L = W$ or $C_L = C_{Lh}$. There can be no more acceleration because the plane is flying horizontally with the throttle entirely open.

(3) If the value of C_D in the point of intersection is smaller than the value mentioned in Case (1), flying is possible and an excess of engine power is available for climbing and acceleration, since, in this case, the coordinates of the point of intersection of circle and polar curve satisfy Eq. (7).

If the drag coefficient C_D is known, it is a simple matter to determine the climbing speed $C = V \sin\theta$ in the usual manner.

Sin θ can also be read from Fig. 3.

$$\frac{A\eta(\text{hp.})}{Vqf} - \left(\frac{W}{gqf}\right)\left(\frac{dV}{dt}\right) = C_D + C_C \quad (13)$$

In this equation $(A\eta\ (\text{hp.})/Vqf) - (W/gqf)\ (dV/dt)$ is regarded as the total available drag coefficient for flying and climbing and, since C_D is the drag coefficient of the plane corresponding with the speed V and the climbing angle θ, C_C can be regarded as the drag coefficient available for climbing, so that for the rate of climb

$$CW = C_C qfV \text{ or } C = V(C_C/C_{Lh})$$

and

$$\sin\theta = C_C/C_{Lh}$$

The angle θ can be immediately read from the figure.

Discussion

(1) Considering Eq. (9), it is clear that the place of the center of a circle is dependent on two terms, of which $A\eta(\text{hp.})/Vqf$ in a chosen speed is known but the second term is not. It can be assumed that the best rate of climb occurs when D/C_D is constant and when q is constant, so that dV/dt can be found as a function of ρ and t. This, however, does not give an easy solution because, before knowing C as a function of t, it is difficult to express ρ as a function of t.

However, the approximate rate of climb can be determined, assuming that there will be no acceleration, in which case V can be found as a function of t, which is sufficiently satisfactory for the construction of the real curve of the rate of climb.

(2) In the preceding consideration a chosen speed is always mentioned. This chosen speed is a function of the $C_D - C_L$ curve and the propulsive efficiency. It is evident, however, that the best rate of climb will only occur when flying with the same airplane but with an assumed weight L at a speed that does not much differ from the speed with a minimum effective propeller horsepower, in which case $C_D/C_L^{3/2}$ is a minimum.

If η is known or sufficiently valued, the speed in question, with minimum horsepower, can be found approximately from the equations

$$\tfrac{1}{2}\, C_L\, V^2 f = G\cos\theta \text{ and}$$

$$\tan\theta = [A\eta(\text{hp.})/VqfC_L] - (C_D/C_L)$$

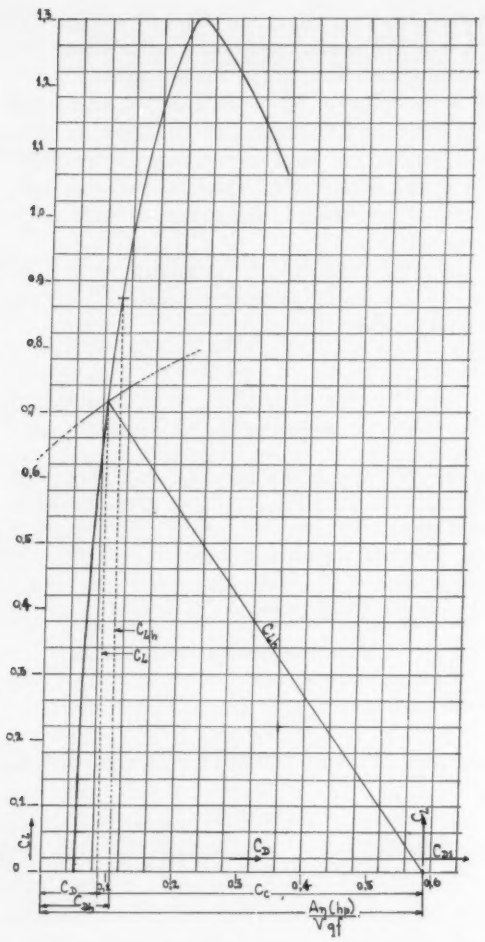

FIG. 2. Construction of C_C—no acceleration assumed.

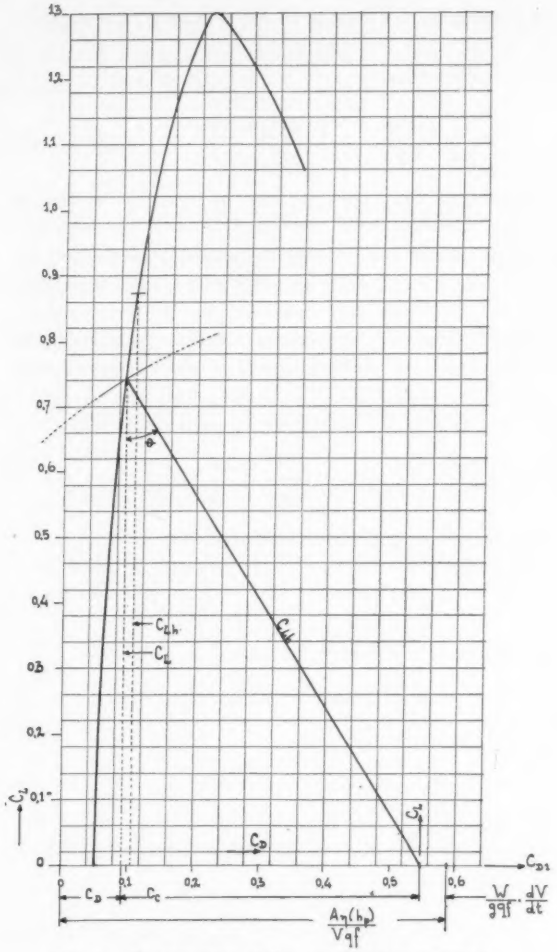

FIG. 3. Construction of C_C—acceleration assumed.

and the values of C_L and C_D, for which $C_D/C_L^{3/2}$ is a minimum. The speed found in this way has to be corrected with respect to the course of the propulsive efficiency.

PROCEDURE

(1) Determine the best speed for climb.

(2) Plot in the C_L–C_D curve for the whole airplane the point:

$$C_D = \frac{A\eta(\text{hp.})}{Vqf}, \quad C_L = 0 \text{ (see Fig. 2)}$$

(3) Determine the value of C_{Lh}, according to the speed V, the air mass density ρ and the weight of the airplane W.

(4) Describe a circle with C_{Lh} as the radius and the point determined in item (2) as a center.

(5) Determine the point of intersection of the circle and the C_L–C_D curve.

(6) Calculate from the figure the value of C_C according to Eq. (13) assuming that there is no acceleration.

(7) To find the climbing speed C, multiply C_C by V and divide by C_{Lh}.

(8) Perform this at the various intervals of heights. Correlate in each interval the rate of climb according to the acceleration.

(9) Determine, with the help of the values found, the value of $(W/gqf)\ (dV/dt)$.

(10) Plot in the C_L–C_D curve the point

$$C_D = \frac{A\eta(\text{hp.})}{Vqf} - \left(\frac{W}{gqf}\right)\left(\frac{dV}{dt}\right), \quad C_L = 0 \text{ (see Fig. 3)}$$

(11) Continue with the same process as described in items (4) through (7), with the point determined in item (10) as the center of the circle. Note the value C_C is now given as:

$$C_C = \frac{A\eta(\text{hp.})}{Vqf} - \left(\frac{W}{gqf}\right)\left(\frac{dV}{dt}\right) - C_D$$

(*Continued on page 57*)

Space Limitations and Optimum Conditions in Aircraft Spring Design

RICHARD H. CARTER*

United Aircraft Corporation

SUMMARY

The effect of space limitations on spring performance is analyzed and leads to optimum design formulas for the three most common types of aircraft springs—i.e., tension, compression, and torsion springs. Using the formulas thus derived, for a given allowable stress the relationship between the space limitations, the maximum load obtainable, and the corresponding wire size can be found immediately. In addition, the process of spring design becomes direct and eliminates trial-and-error methods.

GENERAL

IN PRACTICAL AIRCRAFT spring design, the designer is asked to specify a spring that will fulfill certain requirements. These requirements may vary somewhat but are usually ramifications of the general problem that the spring must do a certain job yet conform to the available space. The procedure usually employed is "trial and error." The designer uses the various formulas and charts and by intelligent guessing tries to find a combination of the variables which will meet the requirements. But often, when the spring requirement exceeds, or is just within, design possibilities, this is a tedious process.

To improve this procedure, certain optimum conditions are developed in this paper. Given a limited space, the use of these conditions affords direct calculation of maximum performance. Thus, if the requirements are too stringent for proper spring design, this may be quickly detected. And as the most efficient spring design is given by these formulas, any surplus weight or space caused by nonoptimum design is eliminated.

Besides the applications to efficient spring calculation, the airplane designer who wishes to incorporate a spring in a unit can immediately calculate the minimum space for proper spring operation without actually having a spring designed. This should eliminate the complications that arise later when it is found that inadequate space has been left for the spring.

To develop these optimum conditions, the maximum load as determined by the allowable stress formula is equated to the load as determined by the formula in terms of the physical characteristics of the problem (i.e., the outside diameter, maximum deflection, etc.). Various manipulations are then performed to obtain the results in the desired forms. The accompanying alignment charts are constructed for stresses normally encountered in aircraft spring design and reduce the calculations to a minimum.

Although the optimum design conditions for the most common general cases are presented in the main analysis, particular problems with various modifications may be solved by logical extensions of the formulas. Important examples at the end of the paper indicate this procedure; the last example is particularly important since it indicates the general approach to certain problems in spring design where the weight must be a minimum.

Received September 22, 1942.

* Structural Research Engineer, Vought-Sikorsky Aircraft Division.

EXTENSION SPRING ANALYSIS

The formulas usually used in spring design are

$$P_{max.} = \pi d^3 S/8K_1D$$

and

$$P_{wkg} = fGd^4/8nD^3$$

where

$$K_1 = \text{Wahl's factor} = 1 + 0.015\left(\frac{d}{D}\right)\left(\frac{91D - 41d}{D - d}\right)$$

S = stress in wire
G = torsional modulus of elasticity
D = mean diameter of coils (D_o = outside diameter)
h = solid heighth of coils
d = wire diameter
f = deflection
n = number of coils

Equating $P_{max.}$ and P_{wkg} introduces optimum conditions on the variables; solving for d gives

$$d^2 = S\pi nD^2/K_1fG \qquad (1)$$

To eliminate n and introduce h, the optimum relation that $n = h/d$ is used; Eq. (1) then becomes

$$d = D\sqrt{S\pi h/K_1fG} \qquad (2)$$

K_1 is a function of D and d but is too complicated to handle conveniently. Hence, an approximation, $K_1' = [5D/(5D - 3d)]^2$, is used. (K_1' is accurate within 1 per cent in the range $4 < (D/d) < \infty$.)

Substituting K_1' for K_1 in Eq. (2) gives

$$d = 5D/(3 + 5\sqrt{Gf/S\pi h}) \qquad (3)$$

Substituting $(D_o - d)$ for D in Eq. (3) gives

$$d = D_o/(1.6 + \sqrt{Gf/S\pi h}) \qquad (4)$$

(This is the optimum design wire size for a given f, h, and D_o.)

d is now eliminated from the given formula ($P_{max.} = \pi S d^3/8K_1D$) and Eq. (4), giving

$$P_{max.} = \left(\frac{\pi S}{8}\right)\left(\frac{1}{K_1 D}\right)\left(\frac{D_o}{1.6 + \sqrt{Gf/\pi Sh}}\right)^3 \quad (5)$$

But K_1D is approximated within 2 per cent in the complete range from $2 < (D/d) < \infty$ by $D_o/[1-(d/2D_o)]$.

$$P_{max.} = \left(\frac{\pi S D_o^2}{8}\right)\left[\frac{1}{(1.6 + \sqrt{Gf/\pi Sh})^3}\right]\left(1 - \frac{d}{2D_o}\right) \quad (6)$$

But $1 - (d/2D_o)$, with $d = D_o/(1.6 + \sqrt{Gf/\pi Sh})$, is equal to

$$(1.1 + \sqrt{Gf/\pi Sh})/(1.6 + \sqrt{Gf/\pi Sh}) \quad (7)$$

By substituting Eq. (7) in Eq. (6),

$$P_{max.} = \frac{\pi S D_o^2 (1.1 + \sqrt{Gf/\pi Sh})}{8(1.6 + \sqrt{Gf/\pi Sh})^4} \quad (8)$$

(This is the maximum load possible for a given f, h, and D_o.)

If the designer is given the spring rate—i.e., P at l_1 and $P_{max.}$ at l_2—and the minimum space for proper operation is desired, it is desirable to have explicit expressions for D_o, f, h, and d in terms of the given values. To retain reasonably simple expressions for these values, an approximation to Eq. (6) is made by assuming $1 - (d/2D_o)$ equal to 0.941 (this assumption is accurate within 3 per cent in the range $4 < (D/d) < \infty$ and exact for $D/d = 7\frac{1}{2}$).

With this assumption,

$$P_{max.} = (\pi S D_o^2/8.5)(1.6 + \sqrt{Gf/\pi Sh})^{-3} \quad (8a)$$

Solving Eq. (8a) for f/h gives the maximum value for f/h for any D_o.

$$f/h = \frac{\pi S}{G}\left[\left(\frac{\pi S D_o^2}{8.5\, P_{max.}}\right)^{1/3} - 1.6\right]^2 \quad (9)$$

where

$$f = (l_2 - l_1)/[1 - (P/P_{max.})]$$

Or solving Eq. (9) for D_o gives the minimum value of D_o for any f/h.

$$D_o = \left[\frac{8.5 P_{max.}}{\pi S}\left(\sqrt{\frac{Gf}{\pi Sh}} + 1.6\right)^3\right]^{1/3} \quad (10)$$

And from the given equation $P_{max.} = \pi d^3 S/8K_1D$,

$$d = \left(\frac{8K_1 D P_{max.}}{\pi S}\right)^{1/3} \quad (11)$$

But

$$(K_1D)^{1/3} = D_o^{1/3}[K_1(1 - d/D_o)]^{1/3}$$

or approximately,

$$(K_1D)^{1/3} = 0.975 D_o[1 + 0.41(d/D_o)]$$

Substituting this in Eq. (11) and solving for d gives the approximate expression

$$d = \frac{4}{3}\left(\frac{D_o P_{max.}}{S}\right)^{1/3}\left[1 + \frac{1}{D_o}\left(\frac{D_o P_{max.}}{S}\right)^{1/3}\right] \quad (11a)$$

(The accuracy is within 1 per cent in the range $2 < (D/d) < \infty$.)

Or approximately,

$$d = (8.5 D_o P_{max.}/\pi S)^{1/3} \quad (11b)$$

(exact for $D/d = 7\frac{1}{2}$).

Compression Spring Analysis

The same analysis as for the extension springs is applicable, except that the two inactive end coils change the relation $n = h/d$. Usually the extra length is considered as $1\frac{1}{2}d$, but various considerations have shown it more practicable to use $2d$ in this analysis.

Calling $h - 2d = h'$, from Eq. (4)

$$d = D_o/(1.6 + \sqrt{Gf/\pi Sh'})$$

But

$$\sqrt{\frac{1}{h'}} = \sqrt{\frac{1}{h}}\left[\frac{1}{1 - (2d/h)}\right]^{1/2}$$

or very nearly

$$\sqrt{1/h'} = [1 + (d/h)]\sqrt{1/h}$$

Therefore,

$$d = \frac{D_o}{1.6 + \sqrt{Gf/\pi Sh}[1 + (d/h)]} \quad (12)$$

It would be possible to solve this quadratic for d, but a simpler expression and one analogous to that in the extension spring analysis is found by putting in the approximate expression for d in the right-hand member. Eq. (2) is used with $n = h/d$, $D = D_o$, and a representative value of $K = 1.41$; these approximations will introduce no practical error for d in the right-hand member. Thus,

$$d = \frac{D_o}{1.6 + \sqrt{Gf/\pi Sh} + (D_o/1.2h)} \quad (13)$$

And by the same procedure as in the extension spring analysis,

$$P_{max.} = \frac{\pi S D_o^2 [1.1 + \sqrt{Gf/\pi Sh} + (D_o/1.2h)]}{8[1.6 + \sqrt{Gf/\pi Sh} + (D_o/1.2h)]^4} \quad (14)$$

From the derivation, it is easily seen that Eqs. (11), (11a), and (11b) are applicable to compression springs without modification. The other expressions for D_o and f/h may be derived, but it is simpler to use the extension spring formulas with the correction that $\sqrt{Gf/\pi Sh}$ in the extension spring formula is equivalent to $\sqrt{Gf/\pi Sh} + (D_o/1.2h)$ for compression springs.

Torsion Spring Analysis

The ordinary formulas are

$$M_{max.} = \frac{Sd^3}{10.2K} \text{ and } M_\theta = \left(\frac{\theta}{360}\right)\left(\frac{Ed^4}{11.25Dn}\right)$$

where

D = mean diameter of coils (D = inside diameter of coils)
n = number of coils
K = Wahl's factor for torsion springs
d = wire diameter
θ = angle of deflection
S = stress in wire
E = Young's modulus

The correct wire size for any maximum moment is given immediately by solving the first of the above equations for d. Thus,

$$d = (10.2KM_{max.}/S)^{1/3} \tag{15}$$

But $K^{1/3}$ is approximately $[1 + (d/5D_i)]$, therefore

$$d = \left(\frac{10.2M_{max.}}{S}\right)\left(1 + \frac{d}{5D_i}\right)$$

or solving for d gives the approximate expression (accurate within 2 per cent from $2 < (D_i/d) < \infty$)

$$d = \left(\frac{10.2\,M_{max.}}{S}\right)^{1/3}\left[1 + \frac{1}{5D_i}\left(\frac{10.2M_{max.}}{S}\right)^{1/3}\right] \tag{15a}$$

Or approximately,

$$d = 2.25(M_{max.}/S)^{1/3} \tag{15b}$$

(exact for $D_i/d = 6$).

To find the optimum wire size as a function of the available space, $M_{max.}$ is equated to M_θ in the given formulas. Solving for d gives $d = 4{,}050DSn/10.2K\theta$.

To find the other optimum relationships, the optimum condition that $n = h/d$ is again used.

But $D/K = (D_i + d)/K$. Since K is approximately $0.965[(D_i + d)/D_i]$, $D/K = D_i/0.965$. Making these two substitutions gives

$$d^2 = \frac{4{,}200S}{10.2E}\left(\frac{D_ih}{\theta}\right) \text{ or } d = 20.3\sqrt{\left(\frac{S}{E}\right)\left(\frac{D_ih}{\theta}\right)} \tag{16}$$

(The error in this assumption is less than 2 per cent in the interval $3 < (D_i/d) < \infty$.)

Eliminating d between Eqs. (15) and (16) gives the equation relating the maximum moment available with a given space and angle of deflection. Thus,

$$M_{max.} = \frac{1}{K}\left(\frac{4{,}200}{E}\right)^{2/3}\left(\frac{S}{10.2}\right)^{5/3}\left(\frac{D_ih}{\theta}\right)^{2/3} \tag{17}$$

$1/K$ is approximately $1 - {}^3/_5(d/D_i)$ and, by substituting Eq. (16) for d, Eq. (17) becomes

$$M_{max.} = 819\left[\frac{S^5}{E^3}\left(\frac{D_ih}{\theta}\right)^3\right]^{1/2}\left[1 - 12\sqrt{\left(\frac{S}{E}\right)\left(\frac{h}{\theta D_i}\right)}\right] \tag{17a}$$

(This approximation is accurate within 1 per cent in the range $3 < (D_i/d) < \infty$.)

Or approximately,

$$M_{max.} = 750\left(\frac{S^5}{E^3}\right)^{1/2}\left(\frac{D_ih}{\theta}\right)^{3/2} \tag{17b}$$

Examples of Special Problems Solvable by Further Analysis

Most spring problems are easily transformed into a form easily solvable by the formulas developed in the general theory, and, with a little experience in their use, the designer can quickly determine the most efficient spring or calculate the space versus performance relation.

However, there are some problems of a more complicated nature which are particularly important to the aircraft spring designer. These are readily solved by extensions of the general principle of optimum design as illustrated by the following examples.

These three examples are for extension spring; however, the methods of analysis are quite similar for the other two types and give analogous results.

Example 1

Given:
Allowable outside diameter (D_o).
Load P_2 at length l_2.
Length $l_1(l_1 > l_2)$.
Length required for end connections (e).
To find:
Lowest load ($P_1 = P_{max.}$) at l_1.
Corresponding wire diameter (d).
From the ordinary formulas,

$$P_{max.} = \pi d^3S/8K_1D \tag{1}$$

$$P_{max.} = \frac{fGd^4}{8hD^3} = \frac{fGd^5}{8D^3(l_1 - f - e)} \tag{2}$$

Eq. (2) introduces two optimum conditions: (1) $h = nd$; (2) $h + e = l_1 - f$.

The third relation between $P_{max.}$ and P_2 is obtained from the spring-rate expression:

$$P_{max.}/f = P_2/(f + l_2 - l_1) \tag{3}$$

Eliminating $P_{max.}$ and f between Eqs. (1), (2), and (3) gives the equation for the wire size:

$$\frac{d^3}{8P_2(D_o - d)} - \frac{l_1 - e}{\frac{\pi S}{K}(l_2 - e) - \frac{Gd^2(l_1 - l_2)}{(D_o - d)^2}} = 0 \tag{4}$$

Although Eq. (4) is a fifth degree equation in d, it is easily solvable by an approximate method, since a reasonably close answer for d may be estimated from the conditions of the problem and the use of the optimum design charts. The equation contains no approximations and, thus, an answer to any degree of accuracy may be obtained. The author has found it ex-

OPTIMUM DESIGN OF TORSION SPRINGS

$$d = \left(\frac{2.06\, D_i H}{\theta}\right)^{1/2} = .0415\,(M_{max})^{1/3}$$

IN THIS CHART, S=150,000 AND E=30,000,000

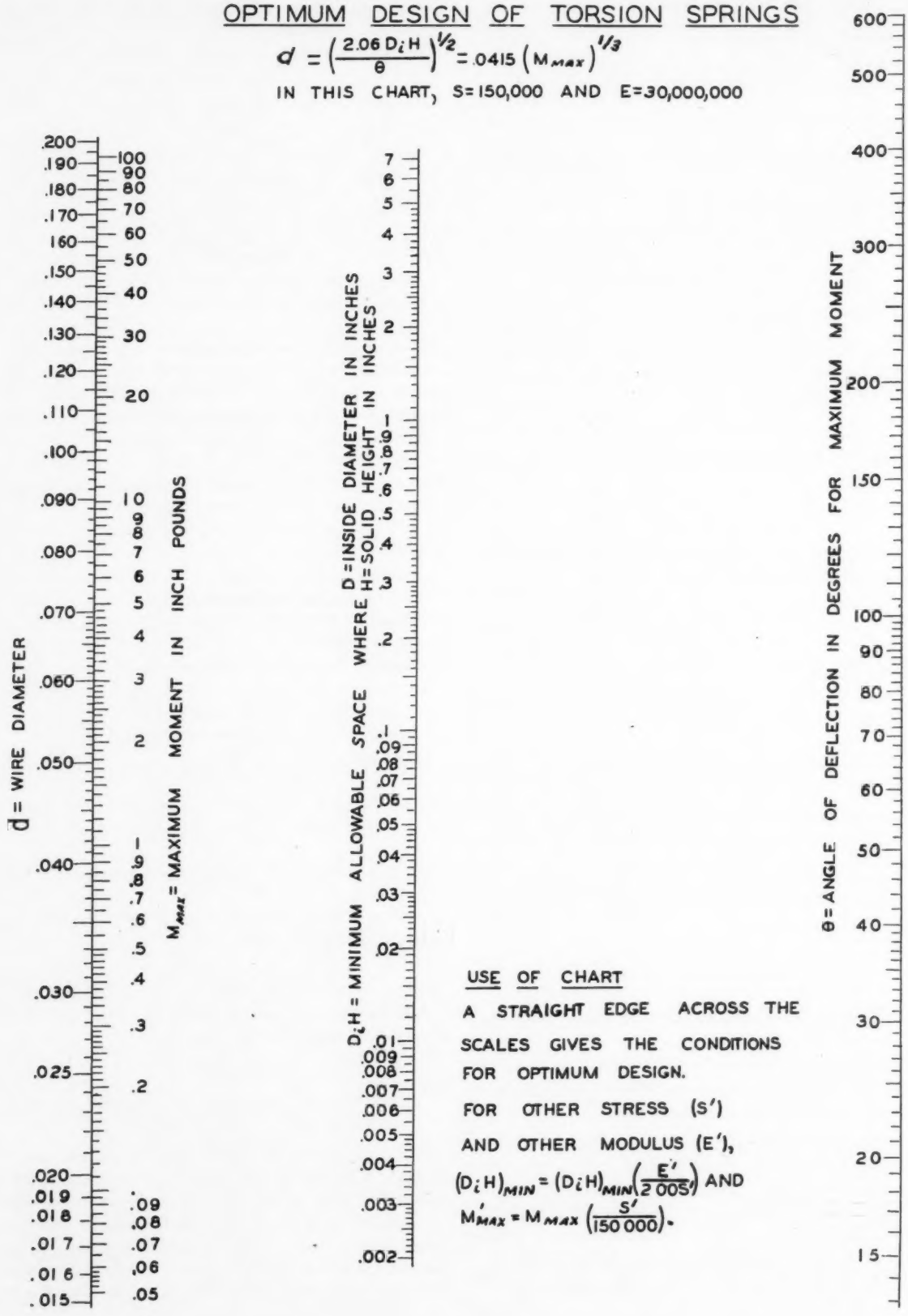

USE OF CHART

A STRAIGHT EDGE ACROSS THE SCALES GIVES THE CONDITIONS FOR OPTIMUM DESIGN.

FOR OTHER STRESS (S') AND OTHER MODULUS (E'),

$(D_i H)_{MIN} = (D_i H)_{MIN}\left(\frac{E'}{2\,005'}\right)$ AND

$M'_{MAX} = M_{MAX}\left(\frac{S'}{150\,000}\right)$.

OPTIMUM DESIGN OF EXTENSION OR COMPRESSION SPRINGS

$$P_{MAX} = 177 D_o^2 \frac{(.182 + \sqrt{f/h})}{(.264 + \sqrt{f/h})^4} \quad \text{AND} \quad d = .0306 \left(P_{MAX} D_o\right)^{1/3}.$$

FOR COMPRESSION SPRING DESIGN f/h IN THE CHART IS EQUIVALENT TO $\left(\sqrt{f/h} + D_o/7h\right)^2$ FOR COMPRESSION SPRINGS.

IN THIS CHART S = 100,000 AND G = 11,500,000.

FOR OTHER STRESS (S') AND OTHER MODULUS (E')

$(f/h)' = \left(\frac{115 S'}{G'}\right) f/h$ AND $\left(D_o P_{MAX}\right)' = \left(\frac{100{,}000}{S'}\right)\left(D_o P_{MAX}\right)$.

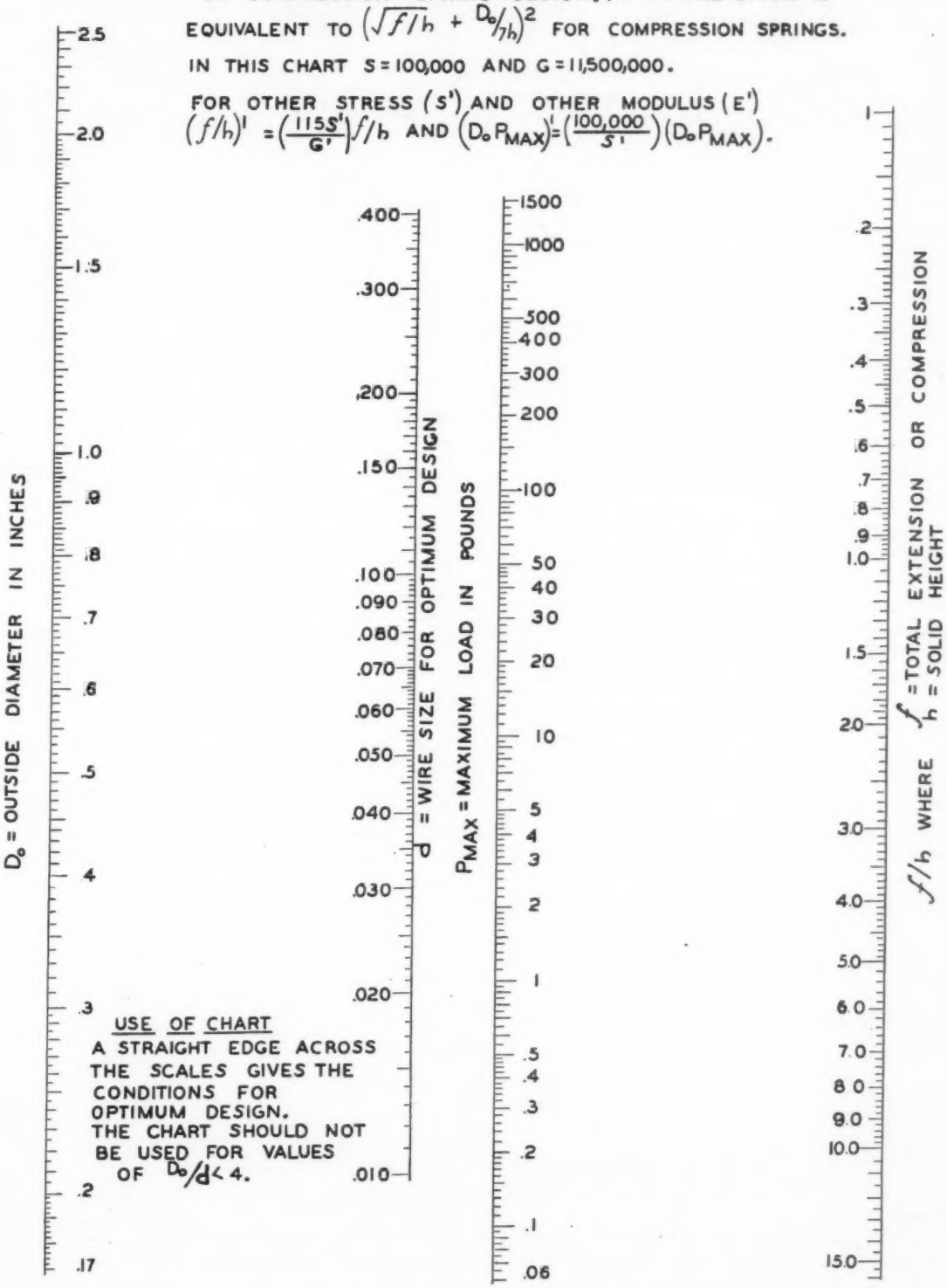

USE OF CHART

A STRAIGHT EDGE ACROSS THE SCALES GIVES THE CONDITIONS FOR OPTIMUM DESIGN. THE CHART SHOULD NOT BE USED FOR VALUES OF $D_o/d < 4$.

pedient to set up forms for computing residuals for the selected values of d and then roughly plot these residuals against d; where the residual is zero gives a close approximation for d. Thus, the correct wire diameter is easily found in about 15 min., and the designer knows that the answer is the best possible solution to the problem.

An explicit expression for $P_{max.}$ would be complicated, so the quickest way to find $P_{max.}$ is by substitution of the optimum wire diameter in Eq. (1).

Example 2

The result of the following analysis will often be of use as an optimum design condition.

Given:

Allowable outside diameter (D_o).

Length l_2.

Length l_1 ($l_1 > l_2$).

Length required for end connections (e).

To find:

The wire diameter (d) which will give the maximum load, P_2 at l_2 without overstressing the spring at l_1, and the corresponding total extension (f).

Solving for P_2 in Eq. (4) gives

$$P_2 = \frac{1}{8(l_1-e)} \times \left[\frac{\pi S}{K_1}(l_2 - e)\frac{d^3}{D_o - d} - G(l_1 - l_2)\frac{d^5}{(D_o - d)^3}\right] \quad (4a)$$

The maximum value of P_2 is found by setting the derivative of P_2 with respect to d equal to zero.

Wahl's factor (K_1) must be taken into account since it is a function of d. Using

$$K_1 = 1 + 0.015\left(\frac{d}{D_o - d}\right)\left(\frac{91D_o - 132d}{D_o - d}\right)$$

gives

$$\frac{\partial K_1}{\partial d} = \frac{1.4D_o}{(D_o - 2d)(D_o - d)}$$

to a good approximation.

Using this value of $\partial K_1/\partial d$ in the expression for $\partial P_2/\partial d = 0$ gives

$$\frac{0.6\pi S(l_2 - e)}{G(l_1 - l_2)} = A = \frac{K_1}{[(D_o/d) - 1]^2} \times \left(\frac{(D_o/d) - 0.4}{D_o/d - 0.667 - \dfrac{0.465}{K_1[1 - (2d/D_o)]}}\right) \quad (5)$$

The values of $(l_1 - l_2)/(l_2 - e)$ (see Fig. 1) are readily plotted against D_o/d giving a convenient method of calculation.

A good approximation for the value of f to give the maximum P_2 without calculating the wire diameter may be found by eliminating d and D from Eqs. (1), (2), and (3) giving P_2 in terms of f. Assuming K_1 a constant and setting $\partial P_2/\partial f = 0$ gives

$$f = \frac{(l_1 - l_2)(l_1 - e)}{(l_1 - 0.4l_2 - 0.6e)} \quad (6)$$

the value of f obtained being somewhat high.

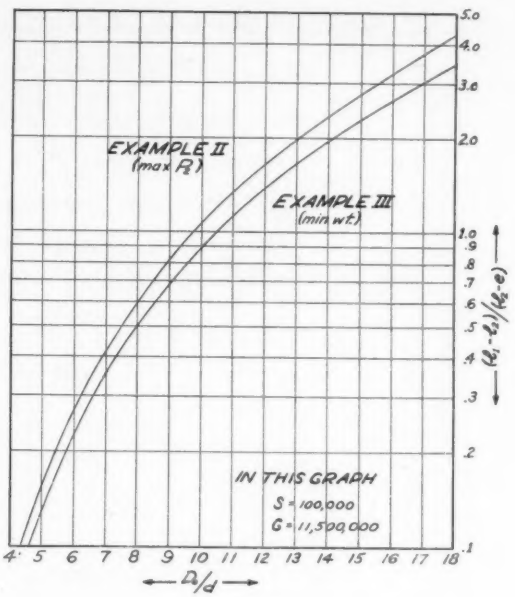

FIG. 1.

Example 3—Optimum Design with Respect to Weight

In Example 2, the wire size, solving the given problem with the specified space limitations, is found by Eq. (4). Often in aircraft spring design, the weight limitations and not the space limitations are critical. In many cases there is an optimum design with respect to the weight, as is illustrated by the following example.

Given:

Load P_2 at length l_2.

Length $l_1(l_1 > l_2)$.

Length required for end connections (e).

To find:

Lowest load ($P_1 = P_{max.}$) at l_1 consistent with the corresponding wire diameter (d) and coil diameter (D) combination giving the lowest weight.

From Eq. (4), $(D_o - d = D)$

$$d^3\left[\frac{\pi S(l_2 - e)}{K_1} - \frac{G(l_1 - l_2)d^2}{D^2}\right] - 8P_2D(l_1 - e) \quad (7)$$

But the weight of a spring (neglecting the inactive portion) is proportional to the cross section of the wire multiplied by the length. Or,

$$W = (\text{constant})d^2nD = (\text{constant})dhD(n = h/d)$$

Therefore, the quantity (dD) is to be minimized (since h is a constant) where d and D are restricted by Eq. (7).

Using the Lagrangian multiplier (λ) method to obtain this minimum value of dD and using

$$\partial K_1/\partial d = 1.4/(D_o - d)$$

and

$$\partial K_1/\partial D = 1.4d^3/D(D - d)$$

as approximations for the derivatives of K_1, the two equations for λ become

$$D + \lambda d^2\left[\frac{3\pi S(l_2 - e)}{K_1}\left(1 - \frac{0.467d}{K_1(D-d)}\right) - \frac{5d^2G(l_1 - l_2)}{D^2}\right] = 0$$

$$d + 2\lambda\left[\frac{0.7\pi S(l_2 - e)d^4}{K_1^2(D-d)D} + \frac{G(l_1 - l_2)d^5}{D^5} - 4P_2(l_1 - e)\right] = 0$$

Eliminating λ and calling $A = (\pi S/K_1)(l_2 - e)$, $B = 2G(l_1 - l_2)$, and $C = 16P_2(l_1 - e)$ gives the equation

$$7B(d/D)^2 - C(D/d^3) = 6AR \qquad (8)$$

where R is nearly equal to $1 - 0.9(d/D)$.

Rewriting Eq. (7) gives

$$B(d/D)^2 + C(D/d^3) = 2A \qquad (9)$$

Eqs. (8) and (9) are linear in $(d/D)^2$ and D/d^3; solving for these quantities gives

$$\left.\begin{aligned}(d/D)^2 &= (A/B)[1 - (0.7d/D)]\\ D/d^3 &= (A/C)[1 + (0.7d/D)]\end{aligned}\right\} \qquad (10)$$

To find the value of D/d, a plot is made (see Fig. 1) of D_o/d against $(l_1 - l_2)/(l_2 - e)$. With this value, d is found from the combination of Eqs. (10); i.e., from

$$d^2 = (C/A)(D/d)/[1 + (0.7d/D)] \qquad (11)$$

The Alignment Charts

These charts are primarily intended for use as an aid in estimates and as a check on the formula calculations. However, as all but the most exact spring design problems do not require a design accuracy within 5 per cent, the charts alone are usually sufficient for calculation. In the author's own experience, these have been a great aid in nearly every spring design problem encountered.

(*Continued from page 50*)

As may be seen from the foregoing, the method described is extremely simple but, assuming that the C_L–C_D curve for the whole airplane is drawn accurately, more precise than the usual methods. With most of these methods, continuation of the calculation of the rate of climb curves at speeds under the minimum horizontal speed of the airplane is not possible. And, as the calculations show, it is possible to fly under the so-called minimum speed when climbing. The way in which the acceleration is taken into account is only a more exact repetition of the work already done in determining the rate of climb in a first approximation, which is already more accurate than that followed in most of the usual methods.

References

[1] Phillips, F. C., *A Kinetic Energy Correction to Predicted Rate of Climb*, Journal of the Aeronautical Sciences, Vol. 9, No. 5, pp. 172–174, March, 1942.

[2] Otten, G., *A New Method for Calculating the Climbing Speeds of Aeroplanes of Great Climbing Capacity*, Journal of the Royal Aeronautical Society, Vol. 39, pp. 133–142, February, 1935.

Dynamics of Constant-Speed Propellers

HERBERT K. WEISS*

Camp Davis

SUMMARY

A theoretic investigation of the performance of constant-speed propeller controls, operating with various types of anticipatory components and several classes of lag, is undertaken over the performance range of the airplane. The effect of aerodynamic parameters of the propeller on the performance of the overall system is established. The advantage of nonlinear control characteristics is noted and demonstrated by calculation of control response for a typical combination of propeller, engine, control, and airplane. A number of charts are presented in dimensionless form, giving the propeller derivatives involved in control design. Charts showing stability requirements for a control system subject to both first- and second-order lag are supplied, as are charts for stability determination of control systems with constant time lag.

INTRODUCTION

IT IS DESIRABLE to maintain constant propeller and engine speed for airplanes under changing conditions of flight.[1] This regulation is obtained in conventional designs by varying propeller blade angle according to some function of the speed error. The control consists of an element capable of measuring the speed error and its integral or derivatives and a servomechanism capable of moving the propeller blade in accordance with the indication of the error sensitive element. Design details of successful controls are available in the literature.[2, 3]

The problem of control design is somewhat complicated by the variation of the aerodynamic parameters of the propeller over the operating range of the control. Since it is customary to keep the sensitivity of the control invariant with airplane velocity, altitude, and engine torque, while change in propeller torque with blade angle and propeller speed varies with forward velocity, density, and power coefficient, it is possible for a control that is perfectly satisfactory for one flight condition to hunt undesirably at another.

Although the propeller and control constitute a nonlinear system with coupling factors, damping and spring coefficients functions of the independent variables, it is possible to assume constancy of the principal parameters by restricting control motion to small displacements. Response characteristics can then be determined by separately examining points distributed over the region of use of the control.

PROPELLER EQUATIONS

Assuming that regulation of propeller speed is to be obtained by control of propeller blade angle, the equations of motion for the controlled propeller will be developed. Let

N = propeller speed (r.p.s.)
n = change in propeller speed from the desired speed (r.p.s.)
β = blade angle (degrees)
β_1 = change in blade angle (degrees)
V = forward speed of the airplane (m.p.h.)
v = change in forward speed of the airplane (m.p.h.)
Q, Q_e, Q_p = torque, engine torque, propeller torque (ft.lb.)
ΔQ = change in torque (ft.lb.)
I = inertia of the engine-propeller combination, referred to the propeller (lb.-ft.-sec.^{2})

A convention of signs will be chosen by defining a positive torque as one that tends to accelerate the propeller. The acceleration of the propeller is then proportional to the algebraic sum of engine and aerodynamic torques.

Engine torque is a function of several variables—among them, engine speed. Increase of engine torque with speed is greatest on engines with high blower

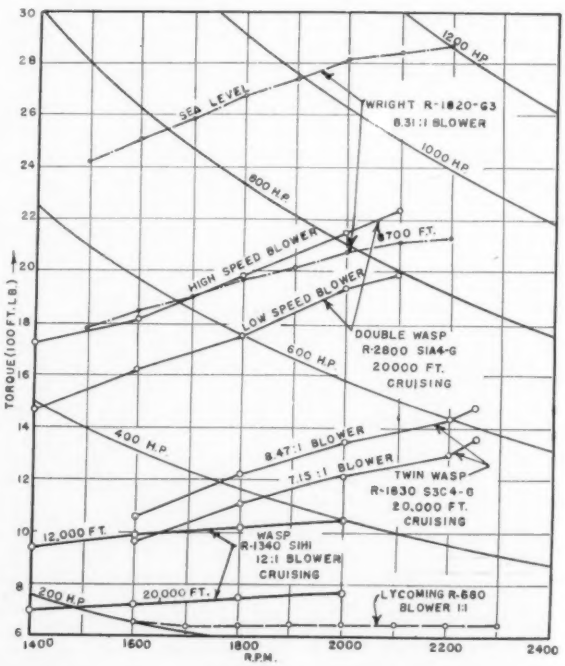

FIG. 1. Torque variation with speed of typical engines.

Received August 18, 1942.

* Antiaircraft Artillery Board.

ratios; unsupercharged engines develop substantially constant torque with changing speed over their normal range of operation. Torque variation for a number of commercially available engines is shown in Fig. 1, where an increase of about 0.80 ft.lb. per r.p.m. is noted for a Double Wasp S1A4-G. Data on high-powered military engines where torque gradient with speed is expected to be greatest are, of course, unavailable for publication. Change in engine torque can be expressed,

$$\Delta Q_e = (\partial Q_e/\partial N)n + \Delta Q_0 \tag{1}$$

where ΔQ_0 includes changes in engine torque from other sources than engine speed, such as throttle setting.

For the propeller

$$Q_p = f(N, V, \beta) \tag{2}$$

and for small changes in the independent variables

$$\Delta Q_p = \frac{\partial Q_p}{\partial N}n + \frac{\partial Q_p}{\partial \beta}\beta_1 + \frac{\partial Q_p}{\partial V}v \tag{3}$$

Acceleration of the propeller is given by

$$I\dot{n} = \Delta Q_e + \Delta Q_p \tag{4}$$

or

$$I\dot{n} = \left(\frac{\partial Q_e}{\partial N} + \frac{\partial Q_p}{\partial N}\right)n + \frac{\partial Q_p}{\partial \beta}\beta_1 + \frac{\partial Q_p}{\partial V}v + \Delta Q_0 \tag{5}$$

The dimensions of Eq. (5) are correct if n is expressed in radians per second. However, it will be more convenient in numerical work to consider n in revolutions per second, in which case inertia I is replaced by $2\pi I$.

The following shortened notation is then adopted,

$$Q_N = 1/2\pi I[(\partial Q_p/\partial N) + (\partial Q_e/\partial N)] \tag{6}$$
$$Q_\beta = 1/2\pi I(\partial Q_p/\partial \beta) \tag{7}$$
$$Q_V = 1/2\pi I(\partial Q_p/\partial V) \tag{8}$$
$$Q_0 = 1/2\pi I(\Delta Q_0) \tag{9}$$

and the equation of motion of the propeller becomes

$$n - Q_N n - Q_\beta \beta_1 = Q_0 + Q_V v \tag{10}$$

A "time constant" for the propeller is defined by assuming the blade angle to be fixed and noting the response of the propeller to a torque Q_0 suddenly applied when the propeller is turning at some constant speed N. The change in propeller speed after the initial transient is

$$n_u = -Q_0/Q_N \tag{11}$$

and the propeller reaches this speed change in an exponential approach

$$n/n_u = 1 - e^{-t/T_p} \tag{12}$$

where

$$T_p = -1/Q_N = \text{propeller time constant} \tag{13}$$

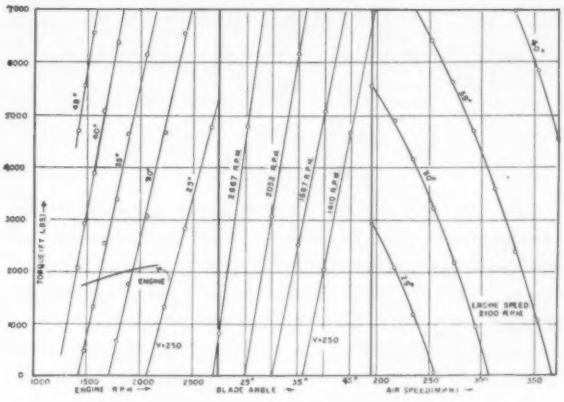

FIG. 2. Aerodynamic torque gradients.

AERODYNAMIC TORQUE DERIVATIVES

The aerodynamic torque derivatives Q_N and Q_β can be calculated for any particular propeller by plotting torque against propeller speed and blade angle in the neighborhood of the point under consideration and noting the respective slopes of the curves. This has been done for a particular case, and the results are plotted in Fig. 2. The engine is a Wright R-1820 G-3, geared 16:11, delivering 840 b.hp. at 2,100 r.p.m. and, 8,700 ft. Propeller diameter is 12.0 ft.; inertia of the propeller-engine combination referred to the propeller shaft is 1,300 lb.-ft.^{2} or 40.4 lb.-ft.-sec.^{2}. Air speed is 250 m.p.h. Then by Eq. (6), the propeller's contribution to Q_N is

$$Q_{Np} = +\left(\frac{1}{2\pi\ 40.4}\right)(-9.0)(60)(16/11) = -3.09 \text{ per sec.}$$

Contribution of the engine torque gradient is

$$Q_{Ne} = +\left(\frac{1}{2\pi\ 40.4}\right)(0.80)(60)(16/11) = +0.28 \text{ per sec.}$$

From Eq. (7)

$$Q_\beta = +\left(\frac{1}{2\pi\ 40.4}\right)(-600) = -2.36 \text{ per deg.-sec.}^2$$

A more general approach to the torque derivatives is through the conventional propeller coefficients. The propeller torque can be expressed in terms of a power coefficient c_p as

$$Q_p = c_p \rho N^2 D^5/2\pi \tag{14}$$

where ρ is air density, D is propeller diameter, and c_p is available from any of the standard references on propeller data. Differentiating Q_p with respect to propeller speed and blade angle and making use of the following notation

$$q_N = \frac{1}{2\pi}\left(2c_p - J\frac{\partial c_p}{\partial J}\right) \tag{15}$$

$$q_\beta = (1/2\pi)\ (\partial c_p/\partial \beta) \tag{16}$$

$$\eta = (1/2\pi I)\ (\rho_{SL} D^5) \tag{17}$$

where ρ_{SL} is standard air density at sea level and $J = V/ND$, it is found that

$$Q_N = q_N \eta N \sigma \tag{18}$$

$$Q_\beta = q_\beta \eta N^2 \sigma \tag{19}$$

Here q_N and q_β are dimensionless parameters depending only on the aerodynamic characteristics of the propeller. η is a dimensionless parameter depending only on propeller diameter and effective propeller inertia. σ is the ratio of actual air density to standard air density at sea level. Fig. 3 shows η computed for a number of propellers of various diameters from data found in propeller literature[4] or supplied by the industry. Engine inertia has not been included in the computations for η in Fig. 3, and a proper increment should be added to account for engine inertia in any particular computation where it is known.

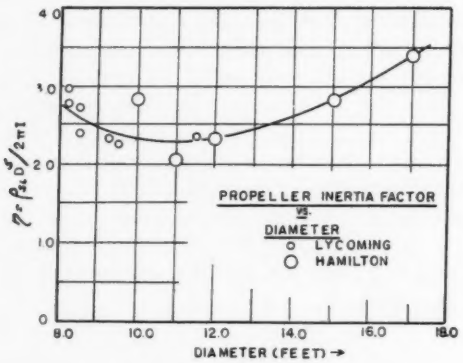

FIG. 3. Propeller inertia factors.

Computation of c_N and q_β has been carried out for two typical propellers with blades of Clark Y section, a two-bladed propeller[5] and a three-bladed propeller.[6] Fig. 4 shows the variation of c_N with J and blade angle. Since propeller torque increases with propeller speed, opposing acceleration, c_N is negative. It is noted that the absolute magnitude of c_N increases rapidly with blade angle and more slowly with J. q_β is shown in Fig. 5. q_β also is negative, increasing in absolute magnitude with J. Variation of q_β with blade angle, however, is neither large nor distinct.

LAWS OF CONTROL

In order to secure control of propeller speed, the blade angle is varied according to some function of speed error. Change in blade angle in turn causes change in propeller torque. If the processes involved between measurement of the speed error and movement of the propeller blade can be expressed in the form of linear differential equations with constant coefficients, the control is considered to be "linear." Actually, an exactly linear control is a rare exception. However, the assumption of linearity can usually be made, subject to whatever restriction to small movements of the control may be required, in order to obtain with readily available mathematical tools results closely if not

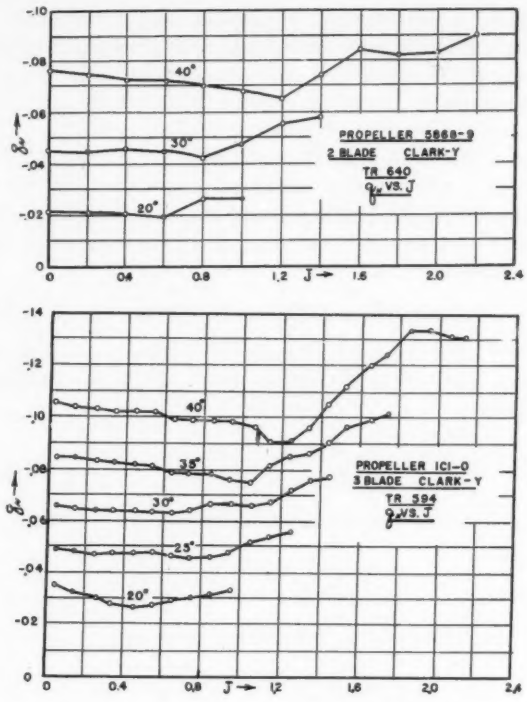

FIG. 4. Variation of q_N with J and blade angle.

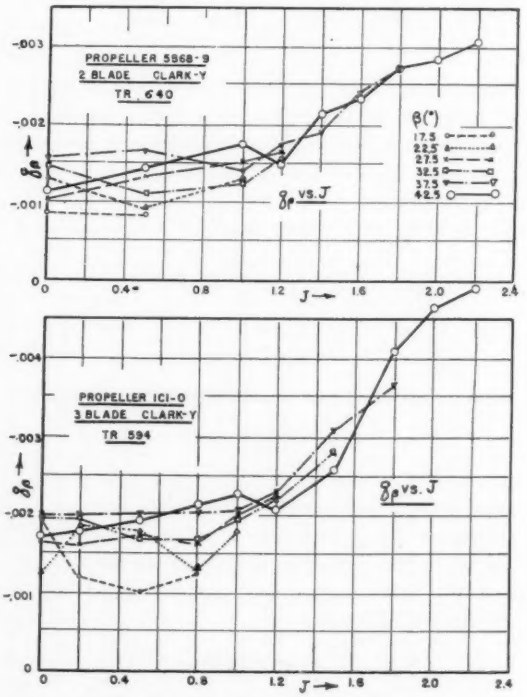

FIG. 5. Variation of q_β with J and blade angle.

exactly, definitive of the actual behavior of the control.

Probably the simplest law of propeller control would be that making the change in blade angle from equilibrium proportional to the speed error. This type of control has been treated at some length in an earlier paper by the writer.[7] It has the disadvantage that with the control adjusted to give the desired propeller speed for some particular engine torque and air speed any departure from these conditions will cause an error in propeller speed which will be present until torque and air speed return to their original values.

By causing the change in blade angle to be proportional to the time integral of the error in propeller speed, the control is given the ability to wipe out steady state errors arising from constant departures of engine torque and air speed from particular reference values. It is frequently further desirable to make the change in blade angle proportional to the derivatives of speed error.

Then assuming temporarily that there is no lag in the control, it is possible to write the most general expression defining response of a linear control as

$$\beta_1 = k_1 \int n\, dt + k_2 n + k_3 \dot{n} + \ldots \tag{20}$$

where

$$k_1 = \partial \dot{\beta}_1 / \partial n \tag{21}$$

$$k_2 = \partial \beta_1 / \partial n \tag{22}$$

$$k_3 = \partial \beta_1 / \partial \dot{n} \tag{23}$$

The physical nature of the integral control will be made more evident by differentiating Eq. (20) once and setting k_2 and higher order components equal to zero. Then

$$d\beta/dt = k_1 n \tag{24}$$

from which it is seen that the integral component makes the rate of change of propeller blade angle proportional to speed error. The Hamilton constant speed control[2] is of this type.

Controlled Propeller

Upon combination of Eqs. (10) and (20), the following expression results.

$$\dot{n}(1 - k_3 Q_\beta) - \dot{n}(Q_N + k_2 Q_\beta) - k_1 Q_\beta n = \dot{Q}_0 + \dot{v} Q_V \tag{25}$$

The following observations can now be made regarding speed error without the necessity for solving Eq. (25).

(1) For constant change in torque Q_0 or constant change in air speed v_0, there is no steady state error in propeller speed.

(2) For constant rate of change of torque $\dot{Q}_0$, there is a steady state error in propeller speed given by

$$n_{ss} = -\dot{Q}_0 / k_1 Q_\beta \tag{26}$$

(3) For constant acceleration dv/dt along the flight path, there is a steady state error in propeller speed given by

$$n_{ss} = -(dv/dt) Q_V / k_1 Q_\beta \tag{27}$$

It is convenient to replace $-Q_V/Q_\beta$ in Eq. (27) by its equivalent from Eqs. (7) and (8)

$$-Q_V/Q_\beta = (\partial\beta/\partial J)/(ND) \tag{28}$$

whence

$$n_{ss} = -(dv/dt)(\partial\beta/\partial J)/(ND k_1) \tag{29}$$

Parameter $\partial\beta/\partial J$ depends only on the aerodynamic characteristics of the propeller. It will be mentioned again later in connection with maximum required blade rate, at which time charts for its determination will be provided.

(4) Damping for the motion represented by Eq. (25) consists of aerodynamic damping from the propeller ($-Q_N$) and "control damping," supplied by the control component that makes change in blade angle proportional to speed error. As indicated by the numerical computation of Q_N, an increase in engine torque with engine speed makes the numerical value of Q_N less negative, and consequently the damping of the system, which is $-Q_N$ is reduced.

(5) Effective inertia of the propeller is reduced by the component of the control which makes blade angle proportional to the first derivative of the speed error. By making $k_3 Q_\beta = 1.00$ the effective inertia of the propeller is made zero. Actually, lag in a physical control would prevent this ideal from being attained, and the control would become unstable, tending to hunt as $k_3 Q_\beta$ approached 1.00.

Damping Ratio

The simplest type of integral control is that which has only a k_1 component and depends for its damping on the aerodynamic damping of the propeller. Defining damping ratio ζ_0 as the ratio of actual damping to the minimum amount required to produce aperiodic motion of the system after a disturbance, it follows from Eq. (25) that for the simple control

$$\zeta_0^2 = -Q_N^2 / 4 k_1 Q_\beta \tag{30}$$

Converting Eq. (30) by substituting q_N and q_β from Eqs. (18) and (19),

$$\zeta_0^2 = -(q_N^2/4q_\beta)(\eta\sigma/k_1) \tag{31}$$

Damping ratio is then decreased by:

(1) Small σ. As altitude increases, the control tends to become more oscillatory.

(2) Small η. Increasing propeller inertia for a given diameter or decreasing propeller diameter for a given inertia will cause the control to become more oscillatory.

(3) Large k_1. A sensitive control, causing large change in blade rate for small speed error, tends to cause oscillatory motion.

(4) Small value of ν, where

$$\nu = \sqrt{-q_N^2/4q_\beta} \tag{32}$$

This ratio involves only general aerodynamic characteristics of the propeller and has been computed for two propellers. Fig. 6 shows ν vs. J for various constant values of $\partial C_s/\partial J$. It was considered desirable to choose $\partial C_s/\partial J$ as a parameter, since, for constant propeller speed and constant engine torque, $\partial C_s/\partial J$ is constant as the airplane changes its forward velocity. This is evident from the expression for the power coefficient C_s

$$C_s = V\sqrt[5]{\rho/PN^2} \tag{33}$$

where P is horsepower.

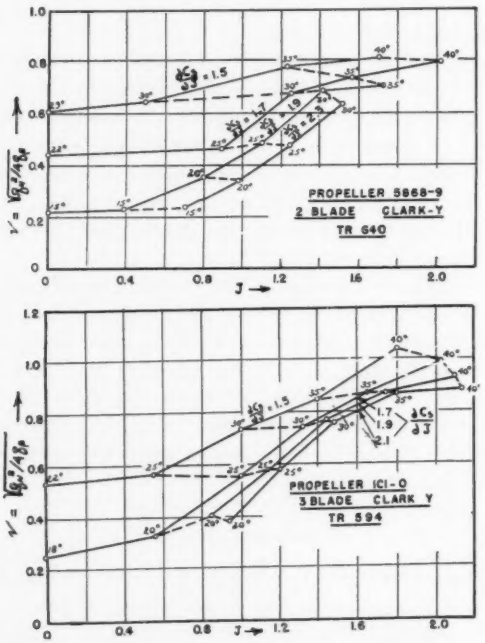

FIG. 6. Variation of ν with J and blade angle.

Change in airplane speed for constant power moves the airplane along a curve of constant $\partial C_s/\partial J$. Change in power for a constant air speed moves the airplane vertically along a line of constant J. The following further conclusions regarding damping of the motion of the controlled propeller can then be drawn with the aid of Fig. 6.

(5) Damping decreases with decreased forward velocity for given engine power and r.p.m.

(6) Damping increases with increased power at a given air speed and r.p.m. for constant engine torque gradient $\partial Q_e/\partial N$.

Since Fig. 6 indicates that aerodynamic damping is least at zero velocity of the airplane or $J = 0$, this region is further investigated in Fig. 7 for propellers of two, three, and four blades.[5] Damping increases with number of blades and, as might be expected, with blade angle.

The curves of ν in Fig. 7, if continued to smaller angles β, would reach a minimum and again rise, in-

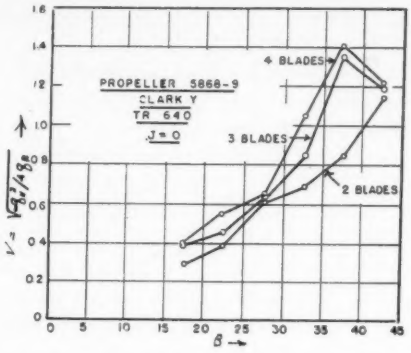

FIG. 7. Variation of ν with blade angle and number of blades.

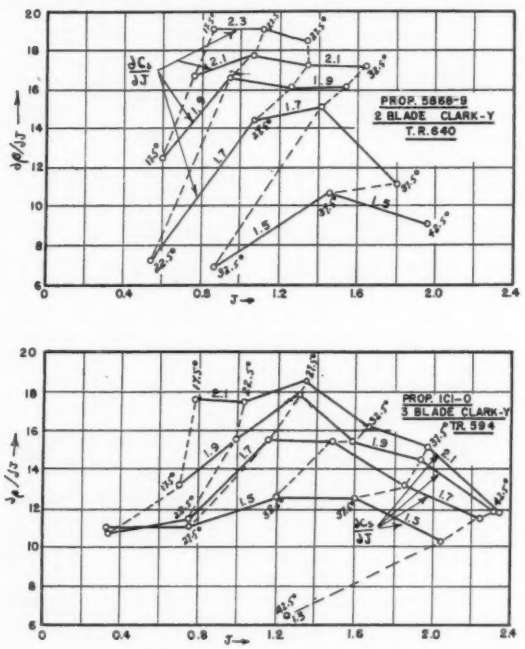

FIG. 8. Variation of $\partial\beta/\partial J$ with J and blade angle.

creasing to infinity since $-q_N$ is always positive; but $-q_\beta$ passes through zero at the blade angle of minimum torque when a change of blade angle in either positive or negative direction causes an increase in torque. In this region the assumption of linearity of the system for small movements no longer holds and, indeed, control in this region is not possible by the system discussed in this paper.

MAXIMUM BLADE RATE

The maximum airplane acceleration with which a control must cope is one of the factors determining the maximum rate of change of blade angle which the control must provide. Disregarding transient requirements, it follows from Eq. (10), when propeller speed error is held negligible, that

$$\dot{\beta}_{max.} = (dv/dt)_{max.}(\partial\beta/\partial J)(1/ND) \tag{34}$$

Again $\partial\beta/\partial J$ depends only on the aerodynamic characteristics of the propeller and is plotted in Fig. 8 for two propellers. It is noted that for a given propeller speed, engine power, and airplane acceleration the maximum blade rate is required as the airplane passes through a region at about $J = 1.30$.

Control Response

The following notation is now introduced

$$\delta = k_2 Q_\beta / Q_N \tag{35}$$

$$\gamma = -k_3 Q_\beta = (1/I)(\partial Q/\partial \dot{n}) \tag{36}$$

Here δ is the ratio of artificially introduced damping to aerodynamic damping already present in the controlled system, and γ is the ratio of change in controlling torque for a unit change in propeller acceleration to change in system torque (inertia) for a unit change in propeller acceleration.

Eq. (25) is now

$$\ddot{n}(1+\gamma) + \frac{\dot{n}}{T_p}(1+\delta) + \frac{n}{T_p^2}\left(\frac{1}{4\zeta_0^2}\right) = \dot{Q}_0 + \dot{v}Q_v \tag{37}$$

The damping ratio of the system with derivative controls is

$$\zeta_s^2 = \zeta_0^2(1+\delta)^2/(1+\gamma) \tag{38}$$

and the solution of Eq. (38) for the error in speed, following a small sudden change in torque ΔQ_0, is

$$\frac{n}{n_u} = Ae^{\frac{-t}{2T_p}\left(\frac{1+\delta}{1+\gamma}\right)} \sin \omega\,(t/T_p) \tag{39}$$

where

$$A = [1/(1+\delta)]\,(2\zeta_s/\sqrt{1-\zeta_s^2}) \tag{40}$$

and

$$\omega = [(1+\delta)/(1+\gamma)]\,(\sqrt{1-\zeta_s^2}/2\zeta_s) \tag{41}$$

For the case of aperiodic motion of the system, when $\zeta_s = 1.00$,

$$\frac{n}{n_u} = [1/(1+\gamma)]\,(t/T_p)e^{-\frac{t}{2T_p}\left(\frac{1+\delta}{1+\gamma}\right)} \tag{42}$$

It should be noted in Eqs. (39) to (42) that the inertia factor $(1+\gamma)$ can always be grouped with the time parameter (t/T_p) to give $[t/T_p(1+\gamma)]$. This indicates that if the damping ratio of the system ζ_s is kept constant the addition of an inertia component γ affects only the time of response of the system and not the error surges. This is not true of the damping component δ, which affects both the response time and amplitude of errors of the system.

Typical solutions of Eq. (39) are given in Fig. 9. For an aperiodic control with only an integral component, the error surge following a sudden change in engine torque is a full 73 per cent of the deviation with no control. Reducing the damping ratio to 0.60 and

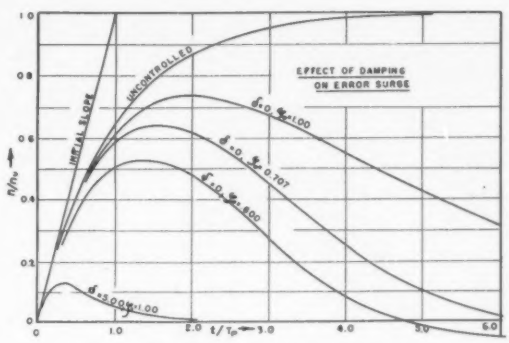

Fig. 9. Effect of damping on error surge.

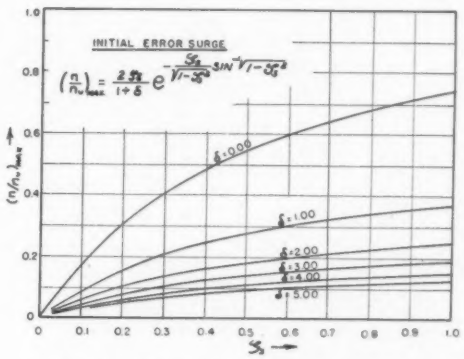

Fig. 10. Magnitude of initial error surge.

making the control oscillatory only reduces the surge to 52 per cent. However, the addition of a control damping component δ of magnitude 5.00 cuts the initial error surge to 13 per cent while retaining aperiodic response for the control. The advantage of the δ component is evident.

Variation of the magnitude of initial error surge with control parameters is obtained by solving Eq. (39) for the time of the error peak and substituting this value of time back into Eq. (39) to determine the maximum value of n/n_u. This is found to be

$$(n/n_u)_{max.} = [2\zeta_s/(1+\delta)]e^{-\frac{\zeta_s}{\sqrt{1-\zeta_s^2}}\sin^{-1}\sqrt{1-\zeta_s^2}} \tag{43}$$

and this expression is plotted in Fig. 10. Merely doubling the available damping by making $\delta = 1.00$ reduces the initial error surge as much as reducing the damping ratio ζ_s to 0.25, and without departing from aperiodicity of the control. Eq. (44) further confirms the observation made earlier that magnitude of error surge after a sudden change in torque is affected only by the damping ratio of the system ζ_s and the damping component of the control δ and not by the inertia component of the control γ.

Lag in the Control

The development so far has considered the propeller control to be without lag—that is, that an error in

propeller speed immediately produced a controlling torque proportional to error, its integral, or derivatives. However, actual controls have lag that is usually undesirable and which may cause the propeller and control to hunt. The incompleteness of the analysis so far is demonstrated by Eq. (37), which indicates that the system represented by control and propeller is always stable and that, when subjected to a transient disturbance, the system will eventually return to a stable position of zero error, provided only that $\zeta_s > 0$. Actual controls are known, however, to be capable of sustained and self-excited oscillations. The theory must then be extended to account for control lag.

The type of lag in a particular control and its order of magnitude will depend on the physical design of the control. A few basic types of lag may be recognized. It is possible to have control lag proportional both to control velocity and acceleration and caused by resilience or "spring" in the control in the presence of damping and inertia, respectively. Constant time lag may also be recognized, in which case the response of the control lags its error impulse always by a constant time interval.

If the desired operation of the control is represented by Eq. (20), introduction of lag proportional to control velocity and acceleration can be written

$$\beta_1 = k_1 \int n\,dt + \ldots - T_c\dot{\beta}_1 - \frac{1}{\omega_n^2}\ddot{\beta}_1 \qquad (44)$$

Notation for the coefficients of $\dot{\beta}_1$ and $\ddot{\beta}_1$ is explained by noting that an additional degree of freedom has been introduced for the control and that, if the control is required to wipe out an arbitrarily applied error β_0 in blade angle in the case of no speed error n and no inertia lag in the control, β_0 is reduced according to the equation

$$\beta = \beta_0 e^{-t/T_c} \qquad (45)$$

so that T_c is the time constant of the control.

Similarly, if $T_c = 0$, the control will hunt about zero after being constrained to depart β_0 from equilibrium according to the expression

$$\beta = \beta_0 \cos \omega_n t \qquad (46)$$

whence ω_n is the "natural undamped frequency" of the control.

It is further desirable to establish two dimensionless lag parameters based on T_c and ω_n as

$$\alpha = T_c/T_p \qquad (47)$$

$$\psi = 1/\omega_n T_p \qquad (48)$$

Referring to Eq. (44) the damping ratio of the free control is noted to be

$$\zeta_c = \omega_N T_c/2 = \alpha/2\psi. \qquad (49)$$

Resolving Eqs. (10) and (44) and denoting by p the dimensionless operator

$$p = T_p(d/dt) \qquad (50)$$

the solution for n written in operational notation is

$$n = \frac{T_p(Q_0 + vQ_v)(p^3\psi^2 + p^2\alpha + p)}{p^4\psi^2 + p^3(\psi^2 + \alpha) + p^2(1 + \gamma + \alpha) + p(1 + \delta) + (1/4\zeta_0^2)} \qquad (51)$$

Since Eq. (51) involves the fourth power of p, indicating a differential equation of the fourth order, it represents motion of a physical system which can easily sustain a self-excited oscillation. Applying Routh's rules for stability,[3] it is found that Eq. (51) represents stable motion if all of the coefficients of the differential equation are positive and if

$$4\zeta_0^2 > \frac{(\alpha + \psi^2)^2}{(\alpha + \psi^2)(1 + \alpha + \psi)(1 + \delta) - \psi^2(1 + \delta)^2} \qquad (52)$$

Eq. (52) is general for a control of one degree of freedom with two orders of lag and both integral and derivative components of control. Stability requirements for simpler controls are obtained by letting the proper parameters go to zero. The case of a simple integral control ($\delta = \gamma = 0$) with first- and second-order lag is presented in Fig. 11 where stability boundaries are shown. Fig. 11 shows that when only first-order lag is present the system is stable for all magnitudes of lag, the only requirement being that ζ_0 be greater than 0.50. The addition of second-order lag for a given amount of first-order lag always makes the system less stable, but the converse is not true, Fig. 11 indicating that an unstable system with inertia lag in the control will not always be stabilized by increasing the damping in the control. For the latter case, stabilization can be obtained only by increasing the aerodynamic damping of the propeller ζ_0 or decreasing the inertia lag of the control ψ. Decreasing the first-order lag (control damping) in the presence of second-order lag will eventually cause instability in the form

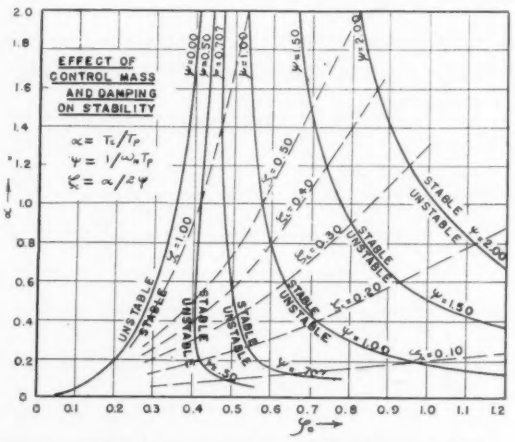

FIG. 11. Effect of control mass and damping on stability.

of hunting at a frequency approaching the natural undamped frequency of the control itself.

To consider the effect of γ and δ on stability, let Eq. (52) be reduced to include only first-order lag. Then

$$4\zeta_0^2 > \alpha/(1 + \alpha + \gamma)(1 + \delta) \tag{53}$$

Stability is increased by positive δ and γ. Since positive δ increases the amount of available damping, its beneficial effect is to be expected. However, for reasons of quick response it is desirable to make γ negative. The limit of permissible negative γ is then fixed by Eq. (53).

Multistage Control

The control considered in Eqs. (51) to (53) involved only one additional degree of freedom. It is possible to have a control consisting of several components in series, each with its own degree of freedom. Such a control might consist of a centrifugal governor with hydraulic power amplification, both governor and oil unit having lag. Consider a control consisting of M units, each subject to first-order lag ($T_1, T_2, \ldots T_M$). The sequence of control equations is

$$\begin{aligned} T_1\dot{x}_1 + x_1 &= c_1 \int n\,dt + \ldots \\ T_2\dot{x}_2 + x_2 &= c_2x_1 \\ T_3\dot{x}_3 + x_3 &= c_3x_2 \\ &\cdot \\ &\cdot \\ &\cdot \\ T_M\dot{\beta}_1 + \beta_1 &= c_Mx_{M-1} \\ T_p\dot{n} + n &= Q_\beta T_p\beta + T_pQ_0 \end{aligned} \tag{54}$$

Noting that

$$c_1c_2 \ldots c_M = k_1 \tag{55}$$

the solution for n in operational notation is

$$n = \frac{T_p(Q_0 + vQ_v)[(p\alpha_1 + 1) \ldots (p\alpha_M + 1)]}{(p\alpha_1 + 1) \ldots (p\alpha_M + 1)(p + 1) + (1/p4\zeta_0^2)} \tag{56}$$

Again making use of Routh's discriminants, the stability requirements for the physical system represented by Eq. (54) can be determined for any particular value of M. This has been done for several cases, and the results are shown in Fig. 12. The case of $M = 2$ is designated as II servo, etc. For $M = 2$, two curves have been plotted, one representing equal lag in the two units and the other curve representing twice as much lag in one unit as in the other. Note that abscissas of Fig. 12 are α_T or the sum of the lag parameters. That is,

$$\alpha_T = \frac{T_1 + T_2 + \ldots + T_M}{T_p} = \alpha_1 + \alpha_2 + \ldots \alpha_M \tag{57}$$

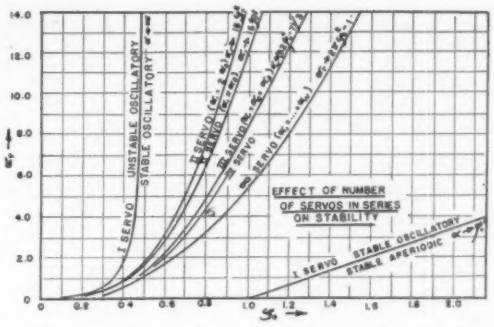

FIG. 12. Effect of number of servos in series on stability.

Then for the case of $M = 2$, stability of the overall system is least for a given total lag α_T when the lag is equally distributed between the two units of the control. A general theorem—stating that when a number of servo units each subject to first-order lag are involved in a control of the type described, the stability is least for a given sum of the lag parameters when the lag is equally distributed among the units—is indicated, but its proof is beyond the scope of the present paper. It suffices to note this fact, and also the additional observation from Fig. 12, that for the case of equal distribution of the lag among the units for a given sum of the lag parameters the stability decreases as the number of units over which the lag is distributed increases.

The limiting case of an infinite number of servo units, each with infinitesimal lag, is obtained by noting that

$$\lim_{M \to \infty} [p(\alpha_T/M) + 1]^M = e^{p\alpha_T} \tag{58}$$

whereupon Eq. (56) becomes

$$n = \frac{pT_p(Q_0 + vQ_v)e^{p\alpha_T}}{e^{p\alpha_T}p(p + 1) + (1/4\zeta_0^2)} \tag{59}$$

The physical meaning of the limiting case expressed as Eq. (59) is clarified by noting that if the simple integral control of Eq. (24) is subject to a constant time lag T such that its response at time t is a function of the speed error at time $t - T$, then

$$\dot{\beta}_t = k_1n_{(t-T)} \tag{60}$$

Following Minorsky's[9] method of treating constant time lag by means of a Taylor's expansion, Eq. (60) becomes

$$\dot{\beta} = k_1(n - \dot{n}T + \frac{1}{2!}\ddot{n}T^2 - \ldots) = k_1ne^{-p\alpha_T} \tag{61}$$

Upon combination of Eqs. (61) and (10), Eq. (59) results. It is then apparent that the response of M servo units in series, with direct coupling and equal first-order lag in each unit, approaches the response of a single unit with constant time lag equal to the sum of all the lag constants as M approaches infinity.

Stability of the limit—that is, of the propeller with a single unit control having time lag of constant mag-

nitude—is determined by assuming that continuous oscillation is present in the control. This indicates that the equation

$$e^{p\alpha_T}p(p+1) + (1/4\zeta_0^2) = 0 \tag{62}$$

has two roots $p = \pm i\omega$. Substituting into Eq. (62) and setting the real and imaginary parts, respectively, equal to zero,

$$\tan \alpha_T\omega = 1/\omega \tag{63}$$

$$\omega\sqrt{1+\omega^2} = 1/4\zeta_0^2 \tag{64}$$

Solving for the minimum value of α_T satisfying Eqs. (63) and (64) for a given value of ζ_0 gives the boundary values between stable and unstable motion, and these have been plotted in Fig. 12. Evidently, for a given lag parameter α_T, the system is least stable when the lag is in the form of a constant time delay in a single servo unit.

Also noted on the curves of Fig. 12 are the simpler relations between α_T and ζ_0 which the curves approach for large values of α_T.

Motion with Lag

Although stability of the controlled propeller with any of the above types of lag present is discovered with reasonable facility by means of Routh's discriminants, it is also desired to know something about the character of the motion should it prove stable. Further investigating the simple integral control with only first-order lag, from Eq. (52) the motion is stable if

$$4\zeta_0^2 > \alpha/(1+\alpha) \tag{65}$$

The boundary between oscillatory and nonoscillatory motion is specified by the requirement for three real roots of the differential equation with at least two real and equal.[10] This is expressed as

$$B^2(1-\alpha)^2 - 2B(1+\alpha)(2\alpha-1)(\alpha-2) - 27\alpha^2 = 0 \tag{66}$$

where $B = 4\zeta_0^2$.

This boundary is plotted in Fig. 12.

The speed error after a sudden change in torque is given by

$$\frac{n}{n_u} = A_1e^{-n(t/T_p)} + e^{-n(t/T_p)}\left(A_2 \sin \omega \frac{t}{T_p} + A_3 \cos \omega \frac{t}{T_p}\right) \tag{67}$$

where

$$A_1 = -(1-2r_2)/[\omega^2 + (r_1-r_2)^2] \tag{68}$$

$$A_2 = -\frac{1}{\omega}\left(\frac{r_2^2 - r_1^2 + r_1 - r_2 - \omega^2}{\omega^2 + (r_1-r_2)^2}\right) \tag{69}$$

$$A_3 = -\frac{(2r_2-1)}{\omega^2 + (r_1-r_2)^2} \tag{70}$$

and $r_1, r_2 \pm i\omega$ are roots of the equation in p

$$p^3\alpha + p^2(1+\alpha) + p + (1/4\zeta_0^2) = 0 \tag{71}$$

Solutions of Eq. (67) are plotted in Fig. 13. In studying the boundary resulting from Eq. (66), two questions might arise: first, the penalty for attempting to maintain aperiodic motion for an actual control with lag; second, the character of the oscillation resulting from provision for only sufficient damping to insure aperiodic response of an ideal control, although the actual control is known to have lag. These two conditions are shown in Fig. 13. Solid curves show error surge of the controlled system with increasing lag as aperiodicity is maintained; dotted curves show response as lag is increased for constant $\zeta_0 = 1.00$.

Numerical Examples

In order to demonstrate typical values of the parameters described in the foregoing series of equations, the response of the typical engine-propeller combination earlier considered has been computed for several conditions. Two major conditions are observed: flight at 250 m.p.h. at 8,700 ft. and initial take-off condition at zero m.p.h. at sea level. Response is calculated in each case for a control with lag constant $T_c = 1.44$ sec. (Cases I and II) and for a control with no lag (Cases Ia and IIa). A simple integral control is assumed with sensitivity $k_1 = 0.985°$ per sec. per r.p.s. To illustrate the effect of changing control sensitivity with blade angle (nonlinear control) the take-off condition has also been recalculated for a nonlinear control (Case III). Forcing function in each case is a sudden 500 ft.lb. change in engine torque. For simplicity the torque gradient of the engine has been neglected. The following parameters are then obtained in computation for the cases with control lag.

Parameter	Case I	Case II	Case III	Source
V	250 m.p.h.	0 m.p.h.	0 m.p.h.	....
Altitude	8,700 ft.	sea level	sea level	....
σ	0.77	1.00	1.00	std. atm.
J	1.27	0.00	0.00	$J = V/ND$
N	24.1 r.p.s.	24.1 r.p.s.	24.1 r.p.s.	....
η	2.33	2.33	2.33	Eq. (17)
C_s	2.14	0.00	0.00	Eq. (33)
$\partial C_s/\partial J$	1.69	1.69	1.69	....
β	29°	18°	18°	N.A.C.A. T.R. 594
q_N	−0.071	−0.022	−0.022	Fig. 4
q_β	−0.0023	−0.0018	−0.0018	Fig. 5
ν	0.740	0.260	0.260	Fig. 6
$\partial\beta/\partial J$	15.5	....	....	Fig. 8
Q_N	−3.08	−1.24	−1.24	Eq. (18)
Q_β	−2.40	−2.43	−2.43	Eq. (19)
T_p	0.324 sec.	0.806 sec.	0.806 sec.	Eq. (13)
Q_0	1.97	1.97	1.97	Eq. (9)
n_u	0.640 r.p.s.	1.59 r.p.s.	1.59 r.p.s.	Eq. (11)
α	4.44	1.78	1.78	Eq. (47)
k_1	0.985°/-sec./r.p.s.	0.985°/-sec./r.p.s.	0.066°/-sec./r.p.s.	....
ζ_0	1.00	0.40	1.55	Eq. (31)

The speed error in r.p.m. has been plotted against time in seconds in Fig. 14. Comparing Cases I and II,

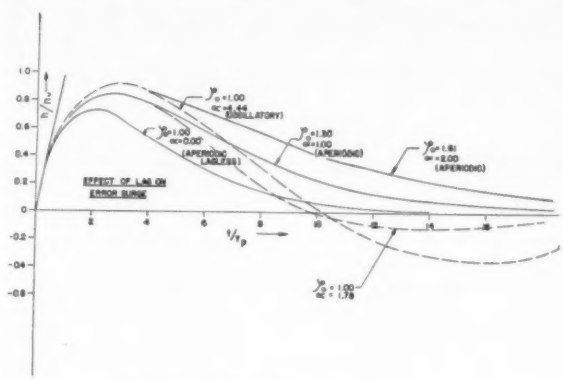

FIG. 13. Effect of lag on error surge.

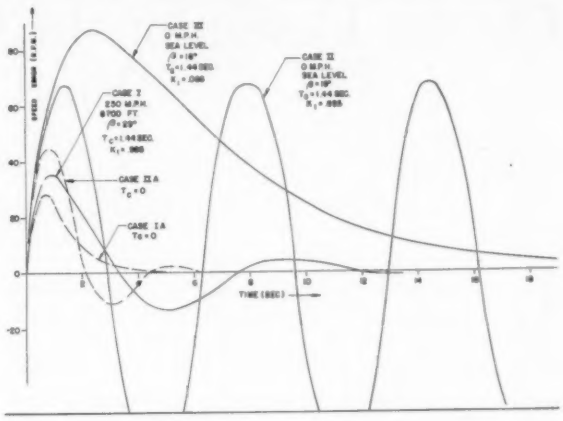

FIG. 14. Computation for actual cases.

it is noted that the control that produces a mild and quickly damped oscillation in flight at 250 m.p.h. still allows a violent and continuous hunting at the take-off condition. Primary cause of the oscillation is the smaller amount of aerodynamic damping available at the lower blade angle required for take-off conditions. When stability is recovered by making control sensitivity proportional to blade angle as in the computation for Case III, the error permitted by the control becomes larger but there is no instability, and for the values chosen in Case III control response is aperiodic.

The harmful effect of control lag is illustrated by comparing the error permitted by the controls with lag in Cases I and II with the errors permitted under exactly the same circumstances by controls of the same sensitivity but without lag in Cases Ia and IIa.

Nonlinear Controls

The observation in the preceding computations—that with a control of constant sensitivity, response of the controlled system may become unstable under conditions where blade angle and aerodynamic damping are low—leads to the proposal that sensitivity k_1 should vary with blade angle β. With the aid of Eqs. (31), (65), and (66) the boundaries in terms of k_1 and β between stable and unstable motion of the propeller-engine system for which the curves of Fig. 14 were computed can be drawn. This has been done in Fig. 15. The permissible control sensitivity decreases rapidly as blade angle decreases. The stable region is larger at sea level than at 8,700 ft. because of the better damping in denser air. Increased lag decreases the size of the stable region, but for this simple first-order lag there is a limit to the unstabilizing effect beyond which sufficient aerodynamic damping is present so that no amount of first-order lag can produce instability.

Since the permissible control, sensitivity for low blade angles as are required at take-off is almost negligible compared with the permissible sensitivity at the blade angles of normal flight, the desirability of a nonlinear control is evident. Noting the small size

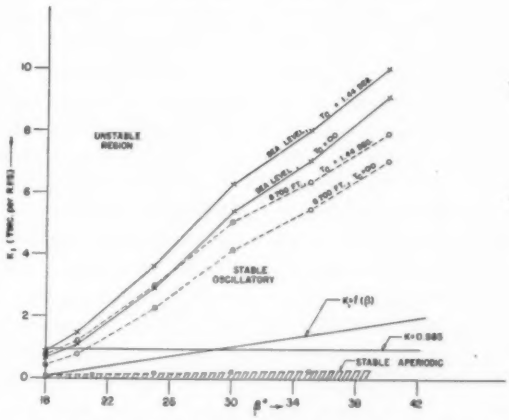

FIG. 15. Stability region for particular propeller-engine combination.

of the nonoscillatory region in Fig. 15, it seems also desirable to permit some overshooting of the control in order to employ sufficient sensitivity to reduce the initial error surge as indicated in Fig. 10.

Conclusions

Specific conclusions regarding the particular components of control and their effects are noted in each section. In general, it may be said that for propellers whose speed is to be controlled by varying the blade angle of the propeller the complete system of control and propeller will be found most stable at high speed and high power, with the possible exception of those cases where increase in engine torque with engine speed on highly supercharged engines may reduce the effective aerodynamic damping and cause hunting. All lag in the control is detrimental, leading to increased error and hunting, especially at low forward speed of the airplane when propeller blade angle is low. Control operation is improved by augmenting the aerodynamic damping of the propeller by a control component which makes change in blade angle proportional to change in

(*Continued on page 70*)

On the Design of the Contraction Cone for a Wind Tunnel

HSUE-SHEN TSIEN*

California Institute of Technology

IN DESIGNING the contraction cone for a wind tunnel, the usual design condition is that the velocity at the end of the cone must be fairly uniform. However, if the curvature of the wall along the flow direction is too large at certain points, local velocities at these points may exceed the uniform velocity at the end of the contraction cone. There are then regions of adverse pressure gradient and the boundary layer may separate from the wall. Furthermore, if the velocity at the end of the contraction cone is very high, say about 0.9 that of the sound, an additional factor enters—namely, the danger of compressibility shock. This danger can be avoided by keeping the velocity of flow below that of sound in the whole field of flow. In the particular case of a contraction cone, the highest velocity is reached at the wall of the cone. Therefore, if the velocity at the wall is made to increase monotonically† from the beginning of the cone to the end of cone, the velocity in the cone will be always less than that of sound, provided that the velocity at the end of the contraction cone is less than the velocity of sound. The pressure along the wall will then be decreasing monotonically. Hence, the danger of boundary layer separation is also avoided.

FORMULATION OF THE PROBLEM

To actually design such a contraction cone using the hydrodynamics of compressible fluids is rather complicated. However, it is substantiated by both theoretic and experimental investigations that the velocity of flow of a compressible fluid can be obtained by increasing the velocity of an incompressible flow with the same boundary by a certain factor. This multiplying factor is a function of the incompressible velocity itself and increases with it.[1] Hence, if a contraction cone is designed for incompressible fluid such that the velocity at the wall increases monotonically from the beginning to the end, the same cone with compressible flow will give a wall velocity that is the product of two monotonically increasing functions and therefore is itself monotone.

Received September 21, 1942.

* Research Fellow in Aeronautics.

† A monotonic increasing function is one in which for every sequence of increasing values of the argument the corresponding values of the function always increase; similarly, a function is monotonic decreasing if its values decrease as the argument increases.

To design such a contraction cone for incompressible flow is, however, much simpler. One can proceed in the following manner:

At the axis of the cone (Fig. 1), i.e., at $r = 0$, assume

$$u = f_0(x) \qquad (r = 0) \tag{1}$$

where u is the velocity in the x-direction. If v is the velocity in the r-direction, by symmetry

$$v = 0 \text{ at } r = 0 \tag{2}$$

Values of u and v or the resultant velocity w can be found for other values of r by using the following fundamental equations of hydrodynamics:

$$\partial v/\partial x - \partial u/\partial r = 0 \tag{3}$$

$$(\partial/\partial x)(ru) + (\partial/\partial r)(rv) = 0 \tag{4}$$

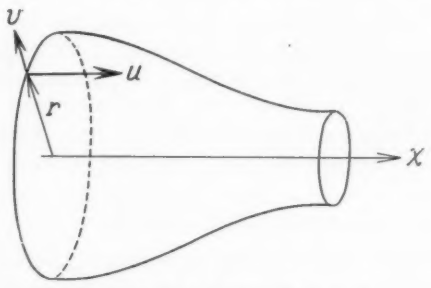

FIG. 1. Flow in a contraction cone.

Eq. (3) is the condition for irrotational flow. Eq. (4) is the continuity equation.

By combining Eqs. (2) and (3), one obtains

$$\partial u/\partial r = 0 \text{ at } r = 0 \tag{5}$$

Hence, u is an even function of r. Similarly, v is shown to be an odd function of r. Therefore, it is appropriate to put

$$u = \sum_{n=0}^{\infty} r^{2n} f_{2n}(x) \tag{6}$$

$$v = \sum_{n=0}^{\infty} r^{2n+1} g_{2n+1}(x) \tag{7}$$

By substituting Eqs. (6) and (7) into Eq. (3) and equating equal powers of r,

$$g'_{2n-1}(x) = 2n f_{2n}(x) \tag{8}$$

where the prime indicates derivative with respect to x. By substituting Eqs. (6) and (7) into Eq. (4) and equating equal powers of r,

$$g_{2n-1}(x) = -\frac{1}{2n} f'_{2(n-1)}(x) \tag{9}$$

Eqs. (8) and (9) give the recurrence relation between the functions f_{2n} as follows

$$f_{2n}(x) = -\frac{1}{(2n)^2} f''_{2(n-1)}(x) \tag{10}$$

Therefore

$$f_{2n}(x) = \frac{(-1)^n}{2^{2n}(n!)^2} f_0^{(2n)}(x) \tag{11}$$

Hence, by substituting these expressions back into Eqs. (6) and (7),

$$u = \sum_{n=0}^{\infty} \frac{(-1)^n r^{2n}}{2^{2n}(n!)^2} f_0^{(2n)}(x) \tag{12}$$

$$v = \sum_{n=1}^{\infty} \frac{(-1)^n 2n r^{2n-1}}{2^{2n}(n!)^2} f_0^{(2n-1)}(x) \tag{13}$$

The resultant velocity w can then be calculated as

$$w = \sqrt{u^2 + v^2} \tag{14}$$

The stream lines are lines of constant values of the stream function ψ defined as

$$\psi(x,r) = \int_0^r ru(x,r)dr \tag{15}$$

By starting from an assigned monotone velocity distribution $u = f_0(x)$ at $r = 0$, the resultant velocity w and the stream lines can be calculated by this procedure. The shape of the contraction cone is then determined by the stream line along which the velocity w still varies monotonically, but further out or for a further increase in the radius r this condition is no longer satisfied. In other words, the shape of the contraction cone is determined by the "last monotone" stream line.

It can be seen that the shape of the contraction cone depends upon the function $f_0(x)$ chosen at the beginning. However, with a plausible assumption of the function, it is believed that a satisfactory design for the contraction cone can be obtained.

It is interesting to notice that the solution in the form Eq. (12) can be easily identified with the well-known Laplace expression for the symmetric potential function

$$u = \frac{1}{\pi} \int_0^{\pi} f_0(x + ir\cos\theta)d\theta \tag{16}$$

However, for practical numerical calculation the series form of Eq. (12) is more convenient.

Solution of the Problem

To carry out the computation, it is assumed that

$$f_0(x) = 0.55 + 0.90 \int_0^x \frac{\sqrt{2\pi}}{1} e^{-(x^2/2)} dx \tag{17}$$

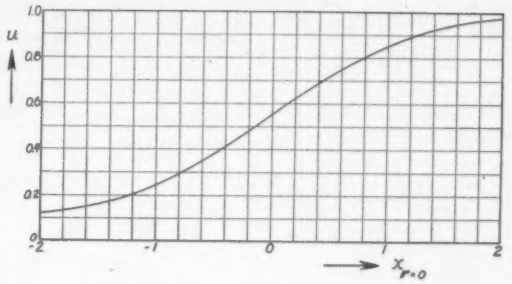

FIG. 2. Assumed velocity u along the axis of the cone as a function of the distance x on the axis.

This distribution of velocity along the axis of the tunnel is shown in Fig. 2. The velocity at the end of contraction cone is here taken as unity. It is seen that the chosen distribution of velocity is quite plausible. Furthermore the derivative of $f_0(x)$ can be easily calculated as follows:

Put

$$\Phi(x) = \frac{1}{\sqrt{2\pi}} e^{-(x^2/2)} \tag{18}$$

then

$$f_0^{(m+1)}(x) = 0.90\Phi^{(m)}(x) \tag{19}$$

But

$$\Phi^{(m)}(x) = \frac{1}{\sqrt{2\pi}} \frac{d^m}{dx^m}(e^{-(x^2/2)})$$

By using the substitutions, $x = \sqrt{2}z$, $x^2/2 = z^2$,

$$\Phi^{(m)}(x) = \frac{1}{\sqrt{2\pi}} \frac{1}{2^{m/2}} \frac{d^m}{dx^m} e^{-z^2} = \frac{(-1)^m}{2^{m/2}} \Phi(x) H_m(z)$$

where $H_m(z)$ is the Hermite polynomial. By means of the recurrence relation between the Hermite polynomials,

$$H_m(z) = 2zH_{m-1}(z) - 2(m-1)H_{m-2}(z)$$

the following recurrence relation between $\Phi^{(m)}(x)$ is immediately obtained

$$\Phi^{(m)}(x) = -[x\Phi^{(m-1)}(x) + (m-1)\Phi^{(m-2)}(x)] \tag{20}$$

The values of $\int_0^x (1/\sqrt{2\pi}) e^{(-x^2/2)} dx$, $\Phi(x)$, $\Phi'(x)$, $\Phi''(x)$, $\Phi'''(x)$, $\Phi^{(iv)}(x)$ are given in many mathematical tables.[2] The higher derivatives can be calculated by using the recurrence relation (20). Then Eq. (19) gives all the required functions for calculating u, and v is given by Eqs. (12) and (13). For each of the series (12) and (13), ten terms are used to give four significant figures. The stream function Ψ is obtained by numerical integration from Eq. (15).

The Results

The stream lines and velocity profiles are plotted in Fig. 3. The part of the stream lines where the velocity exceeds unity, the asymptotic velocity of the cone, is drawn as dotted lines. Therefore, theo-

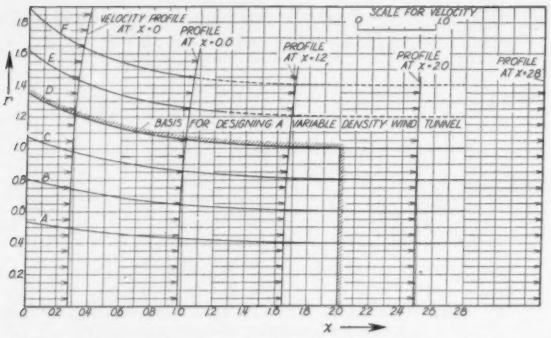

FIG. 3. Stream lines (A B, C, D, E, F) in the meridian x, r plane of the contraction cone together with the velocity profiles at different sections.

retically the "last monotone" stream line must lie inside the line E. However, for the stream line F, the velocity at $x = 1.2$ is 1.032, while at $x = 2.0$ the value is 1.018. This slight excess of velocity will be easily removed by wall friction if this stream line is used as the wall of the contraction cone. In other words, the stream line F can be used as the shape for the contraction cone.

This result has been applied to the design of the contraction cone of a large variable density wind tunnel. The cross section of the contraction cone is not circular but partly circular and partly octagonal. Since this modification must tend to increase the local velocity at some points of the wall, it is thus thought safer to use the stream line D instead of stream line F as the basis for designing the contraction cone. Furthermore, the velocity change from $x = 2.0$ to $x = 2.8$ is negligible. Therefore, the final recommended shape of the contraction cone for this particular wind tunnel is based upon a boundary as marked in Fig. 3.

REFERENCES

[1] von Kármán, Th., *Compressibility Effects in Aerodynamics*, Journal of Aeronautical Sciences, Vol. 8, pp. 337–356, July, 1941.

[2] *See* Burington, R. S., *Handbook of Mathematical Tables and Integrals*, pp. 257–259; Handbook Publishers, Inc., Sandusky, O., 1940.

(*Continued from page 67*)

propeller speed. There seem to be real benefits to be derived in the case of integral or "rate" controls in having control sensitivity decrease with blade angle, thereby assuring close regulation at high speeds and angles and stability at low speeds and angles.

REFERENCES

[1] Caldwell, F. W., Martin, E., Rhines, T. B., and Baker, C. F., *The Constant Speed Propeller, Part I, Its Performance*, S.A.E. Journal, Vol. 40, No. 1, pp. 28–33, January, 1937.

[2] Caldwell, F. W., Martin, E., Rhines, T. B., and Baker, C. F., *The Constant Speed Propeller, Part II, Development of Its Control*, S.A.E. Journal, Vol. 40, No. 1, pp. 33–44, January, 1937.

[3] *Curtiss Constant Speed Propeller*, Aero Digest, Vol. 31, No. 6, pp. 60, 62, December, 1937.

[4] Lampton, G. T., *Testing of Controllable-Pitch Propellers*, A.S.M.E. Trans., Vol. 58, No. 4, pp. 263–266, May, 1936.

[5] Hartman, Edwin P., and Bierman, David, *The Aerodynamic Characteristics of Full-Scale Propellers Having 2, 3, and 4 Blades of Clark Y and R.A.F. 6 Airfoil Sections*, N.A.C.A. T.R. No. 640, 1938.

[6] Theodorsen, Theodore, Stickle, George W., and Brevoort, M. J., *Characteristics of Six Propellers, Including the High-Speed Range*, N.A.C.A. T.R. No. 594, 1937.

[7] Weiss, Herbert K., *Constant Speed Control Theory*, Journal of the Aeronautical Sciences, Vol. 6, No. 4, pp. 147–152, February, 1939.

[8] Routh, E. J., *Advanced Rigid Dynamics*, Chapter VI; The Macmillan Company, London, 1930.

[9] Minorsky, Nicholas, *Control Problems*, Journal of the Franklin Institute, Vol. 232, No. 5, pp. 451–487, November, 1941; No. 6, pp. 519–551, December, 1941.

[10] Dixon, Leonard E., *Elementary Theory of Equations*, p. 33; John Wiley & Sons, New York, 1914.

Induced Drag of a Twisted Wing

H. W. SIBERT*
University of Cincinnati

Introduction

THE FORMULA usually given for the induced drag coefficient of a wing is (p. 7-28[1])

$$C_{D_i} = (1 + \sigma)C_L^2/\pi A \qquad (1)$$

in which C_L is the wing lift coefficient, A the aspect ratio and σ the induced-drag factor. Although valid for an untwisted wing (section zero-lift chords all parallel), Eq. (1) gives incorrect values for a twisted wing. For example, $C_{D_i} = 0$ in Eq. (1) when $C_L = 0$, while the induced-drag coefficient of a twisted wing is never zero.

The correct formula for the induced-drag coefficient of a twisted wing can be derived from the theory of spanwise air-load distribution given in references 1 and 2. In this theory the section lift coefficient C_l at any airfoil section along the span is expressed as a Fourier series, namely (p. 7-29[1])

$$C_l = (m_s c_s/c)(A_1 \sin\theta + A_2 \sin 2\theta + A_3 \sin 3\theta + \ldots) \qquad (2)$$

where c is the chord of the airfoil section; c_s, the chord at the plane of symmetry; m_s, the slope of the section lift coefficient at the plane of symmetry; A_n, a general coefficient of the Fourier series; and θ, the arc cosine of the distance of the airfoil section from the plane of symmetry as a fraction of the semispan. With C_l defined as in Eq. (2), the wing-lift coefficient is (p. 7-28[1])

$$C_L = \pi A u_0 A_1 \qquad (3)$$

where A_1 is the coefficient of $\sin\theta$ in Eq. (2) and $u_0 = m_s c_s/4b$ (p. 7-26[1]), b being the span of the wing. The induced-drag factor σ is defined by the relation (p. 7-28[1])

$$1 + \sigma = (A_1^2 + 2A_2^2 + 3A_3^2 + 4A_4^2 + \ldots)/A_1^2 \qquad (4)$$

where $A_1, A_2, A_3, \ldots$ are the same A's appearing in Eq. (2). The result of substituting in Eq. (1) the values of C_L and $(1 + \sigma)$ given in Eqs. (3) and (4) is

$$C_{D_i} = \pi A u_0^2(A_1^2 + 2A_2^2 + 3A_3^2 + 4A_4^2 + \ldots) \qquad (5)$$

The correct formula for the induced-drag coefficient of a twisted wing can be derived from Eqs. (3), (4), and (5).

Received March 21, 1942.

* Formerly Associate Professor of Mathematics and Aeronautics. At present, Major, U.S. Army Air Forces Reserve.

Twisted Wing

The following analysis treats specifically the case of a wing with a defected flap. With a slight change in notation, the resulting formulas will also be valid for a wing with washout (or washin) at the tips. Let A_{1U}, A_{2U}, A_{3U}, ... be the A's for the untwisted wing (flap closed) at an angle of attack of 1 radian from its zero-lift position. Let A_{1F}, A_{2F}, A_{3F}, ... be the A's for the additional lift due to the flap alone when the $k\delta$ for the flap is one radian. For a twisted wing at an angle of attack of x radians from the zero-lift position of the untwisted wing and with the $k\delta$ of its deflected flap equal to r radians, the corresponding A's are $(xA_{1U} + rA_{1F})$, $(xA_{2U} + rA_{2F})$, $(xA_{3U} + rA_{3F})$, ... The wing-lift coefficient and induced-drag coefficient of this twisted wing are, respectively (Eqs. (3) and (5)),

$$C_L = \pi A u_0(xA_{1U} + rA_{1F}) \qquad (6)$$

$$C_{D_i} = \pi A u_0^2[(xA_{1U} + rA_{1F})^2 + 2(xA_{2U} + rA_{2F})^2 + 3(xA_{3U} + rA_{3F})^2 + \ldots] \qquad (7)$$

Let C_{L_U} and σ_U be, respectively, the wing-lift coefficient and induced-drag factor of the untwisted wing at an angle of attack of x radians from its zero-lift position. C_{L_U} and σ_U can be found from Eqs. (3) and (4), respectively, by replacing each A_n by xA_{nU}.

$$C_{L_U} = \pi A u_0 x A_{1U} \qquad (8)$$

$$1 + \sigma_U = (A_{1U}^2 + 2A_{2U}^2 + 3A_{3U}^2 + \ldots)/A_{1U}^2 \qquad (9)$$

From Eq. (9), σ_U is independent of x and, hence, is constant for all values of C_{L_U}.

Let x_m be the value of x at which C_{D_i} of the twisted wing is a minimum. C_{D_i} is a minimum when $\partial C_{D_i}/\partial x = 0$. Hence, from Eqs. (7) and (9),

$$x_m = rk_m \qquad (10)$$

$$k_m = -(A_{1U}A_{1F} + 2A_{2U}A_{2F} + \ldots)/(A_{1U}^2 + 2A_{2U}^2 + \ldots) = -(A_{1U}A_{1F} + 2A_{2U}A_{2F} + 3A_{3U}A_{3F} + \ldots)/A_{1U}^2(1 + \sigma_U) \qquad (11)$$

By virtue of Eq. (11), the substitution of this value of x_m for x in Eq. (7) gives the following minimum value of C_{D_i}:

$$C_{D_{im}} = \pi A u_0^2 r^2 K_m \qquad (12)$$

$$K_m = (A_{1F}^2 + 2A_{2F}^2 + \ldots) + k_m(A_{1U}A_{1F} + 2A_{2U}A_{2F} + \ldots) = (A_{1F}^2 + 2A_{2F}^2 + 3A_{3F}^2 + \ldots) - k_m^2 A_{1U}^2(1 + \sigma_U) \qquad (13)$$

Expanding Eq. (7),

$$C_{D_i} = \pi A u_0^2[x^2(A_{1U}^2 + 2A_{2U}^2 + \ldots) + 2xr(A_{1U}A_{1F} + 2A_{2U}A_{2F} + \ldots) + r^2(A_{1F}^2 + 2A_{2F}^2 + \ldots)] \quad (14)$$

The result of substituting in Eq. (14) the values of $(A_{1U}^2 + 2A_{2U}^2 + \ldots)$, $(A_{1U}A_{1F} + 2A_{2U}A_{2F} + \ldots)$, and $(A_{1F}^2 + 2A_{2F}^2 + \ldots)$ given in Eqs. (9), (11), and (13), respectively, is

$$C_{D_i} = \pi A u_0^2[(1 + \sigma_U)(xA_{1U} - rk_mA_{1U})^2 + r^2K_m] \quad (15)$$

At this point it will be convenient to introduce the quantities $C_{D_{im}}'$ and $C_{L_{Um}}'$, which are, respectively, the minimum C_{D_i} and the corresponding C_{L_U} when $r = 1$, that is, when the $k\delta$ of the flap is 1 radian. From Eqs. (12), (10), and (8)

$$C_{D_{im}}' = \pi A u_0^2 K_m, \; C_{L_{Um}}' = \pi A u_0 k_m A_{1U} \quad (16)$$

The result of substituting in Eq. (15) the values of xA_{1U}, k_mA_{1U}, and K_m given in Eqs. (8) and (16) is

$$C_{D_i} = (1 + \sigma_U)(C_{L_U} - rC_{L_{Um}}')^2/\pi A + r^2C_{D_{im}}' \quad (17)$$

From Eqs. (8), (10), (12), and (16) it is evident that the terms $r^2C_{D_{im}}'$ and $rC_{L_{Um}}'$ in Eq. (17) are, respectively, the minimum C_{D_i} and the corresponding C_{L_U} when the $k\delta$ of the flap is r radians. This fact checks the validity of Eq. (17), since the minimum value of the first term of Eq. (17) is zero, which occurs when $C_{L_U} = rC_{L_{Um}}'$.

Let x_0 be the value of x for zero wing lift when the $k\delta$ of the flap is r radians. From Eq. (6)

$$x_0 = rk_0, \; k_0 = -A_{1F}/A_{1U} \quad (18)$$

Let $C_{L_{U0}}'$ be the value of C_{L_U} at zero wing lift when $r = 1$—that is, when the $k\delta$ of the flap is 1 radian. From Eqs. (8) and (18)

$$C_{L_{U0}}' = \pi A u_0 k_0 A_{1U} \quad (19)$$

From Eq. (18) it is evident that $rC_{L_{U0}}'$ is the value of C_{L_U} at zero wing lift when the $k\delta$ of the flap is r radians. Hence, if C_L is the wing-lift coefficient when the $k\delta$ of the flap is r radians,

$$C_L = C_{L_U} - rC_{L_{U0}}' \quad (20)$$

The result of substituting in Eq. (17) the value of C_{L_U} given in Eq. (20) is

$$C_{D_i} = (1 + \sigma_U)[C_L + r(C_{L_{U0}}' - C_{L_{Um}}')]^2/\pi A + r^2C_{D_{im}}' \quad (21)$$

where σ_U, $C_{L_{U0}}'$, $C_{L_{Um}}'$, and $C_{D_{im}}'$ are defined by Eqs. (9), (19), and (16). Note that from Eqs. (19) and (16)

$$C_{L_{U0}}' - C_{L_{Um}}' = \pi A u_0 A_{1U}(k_0 - k_m) \quad (22)$$

where k_0 and k_m are defined by Eqs. (18) and (11), respectively.

Example

Find the formula for C_{D_i} for a wing for which the $k\delta$ of the flap is r radians when the A's for the untwisted wing and for the flap alone are those given on pages 7-28 and 7-40, respectively, of reference 1. These A's have been obtained from the procedure outlined in that reference. The even A's were all zero and

$$A_{1U} = 0.6777, \; A_{3U} = -0.0155, \; A_{5U} = 0.0309$$
$$A_{7U} = 0.0009, \; A_{9U} = 0.0043, \; 1 + \sigma_U = 1.0118$$
$$A_{1F} = 0.4598, \; A_{3F} = -0.1302, \; A_{5F} = -0.0495$$
$$A_{7F} = 0.0675, \; A_{9F} = -0.0206$$
$$A_{1U}^2 + 2A_{2U}^2 + 3A_{3U}^2 + \ldots = 0.4647$$
$$A_{1F}^2 + 2A_{2F}^2 + 3A_{3F}^2 + \ldots = 0.3103$$
$$A_{1U}A_{1F} + 2A_{2U}A_{2F} + 3A_{3U}A_{3F} + \ldots = 0.3080$$
$$A = 7.582, \; u_0 = 0.2801 \text{ (pp. 7-24, 7-26)}$$
$$k_0 = -0.4598/0.6777 = -0.67847 \text{ (Eq. (18))}$$
$$k_m = -0.3080/0.4647 = -0.66279 \text{ (Eq. (11))}$$
$$K_m = 0.3103 - 0.66279 \times 0.3080 = 0.1062 \text{ (Eq. (13))}$$
$$C_{L_{U0}}' - C_{L_{Um}}' = \pi \times 7.582 \times 0.2801 \times 0.6777\,(-0.01568) = -0.071 \text{ (Eq. (22))}$$
$$C_{D_{im}}' = \pi \times 7.582 \times 0.2801^2 \times 0.1062 = 0.1980 \text{ (Eq. (16))}$$
$$(1 + \sigma_U)/\pi A = 1.0118/(\pi \times 7.582) = 0.0425$$
$$C_{D_i} = 0.0425\,(C_L - 0.071r)^2 + 0.198r^2 \text{ (Eq. (21))}$$

With this flap deflected 60°, $r = 0.1734$ (p. 7-32[1]).

Hence, for a 60° flap deflection

$$C_{D_i} = 0.0425\,(C_L - 0.0123)^2 + 0.0060$$

Wing with Washout at the Tips

Eq. (21) can be applied to a wing with washout (or washin) at the tips by deleting r and r^2 and letting $C_{L_{U0}}'$, $C_{L_{Um}}'$ and $C_{D_{im}}'$ refer to the effect of the twist alone. Another procedure is to leave Eq. (21) unchanged with $C_{L_{U0}}'$, $C_{L_{Um}}'$ and $C_{D_{im}}'$ referring to the twist alone of a hypothetic wing whose tip chord is twisted 1 radian with respect to the root chord. Then, r would be the actual twist in radians of the tip chord relative to the root chord.

The amount of washout (or washin) at the tips in most airplane wings is not large and its effect on Eq. (21) should be much smaller than the corresponding effect of a 60° deflected flap. Hence, for a wing whose only twist is a washout (or washin) at the tip, little error should result from changing Eq. (21) into

$$C_{D_i} = (1 + \sigma_U)C_L^2/\pi A \quad (23)$$

One would hardly be justified, though, in applying Eq. (23) to a twisted wing having a flap at its maximum deflection.

References

[1] ANC-1(1), *Spanwise Air-Load Distribution*, Army-Navy-Commerce Committee on Aircraft Requirements, April, 1938.

[2] N.A.C.A. T.R. No. 572.